



1 Calcification response of planktic foraminifera to environmental change in the
2 Western Mediterranean Sea during the industrial era

3

4 Thibault M. Béjard^{1*}, Andrés S. Rigual-Hernández¹, José A. Flores¹, Javier P.
5 Tarruella¹, Xavier Durrieu de Madron², Isabel Cacho³, Neghar Haghypour⁴, Timothy
6 Eglinton⁴, Francisco J. Sierro¹

7

8 1. Area de Paleontología, Departamento de Geología, Universidad de Salamanca,
9 37008 Salamanca, Spain

10 2. Université de Perpignan Via Domitia, CNRS, CEFREM, Perpignan, France

11 3. GRC Geociències Marines, Departament de Dinàmica de la Terra i de l'Oceà,
12 Facultat de Ciències de la Terra, Universitat de Barcelona, Barcelona, Spain

13 4. Earth Sciences Department, ETH Zurich, Zurich, 8092, Switzerland

14

15 * *Corresponding author:* Area de Paleontología, Departamento de Geología,
16 Universidad de Salamanca, 37008, Salamanca, Spain. *E-mail address:*
17 thibault.bejard@usal.es.

18 Abstract

19

20 The aim of this work is to investigate the variability of planktic foraminifera
21 calcification in the northwestern Mediterranean Sea on seasonal, interannual and
22 pre-industrial Holocene time scales. This study is based on data from a 12-year-long
23 sediment trap record retrieved in the in the Gulf of Lions and seabed sediment
24 samples from the Gulf of Lions and the promontory of Menorca. Three different
25 planktic foraminifera species were selected based on their different ecology and
26 abundance: *Globigerina bulloides*, *Neogloboquadrina incompta*, and *Globorotalia*
27 *truncatulinoidea*. A total of 273 samples were weighted in both sediment trap and
28 seabed samples. As the traditionally used sieve fractions method is considered
29 unreliable because of the effect of morphometric parameters on the foraminifera
30 weight, we measured area and diameter to constrain the effect of these parameters.
31 The results of our study show substantial different seasonal calcification patterns
32 across species: *G. bulloides* showed a slight calcification increase during the high
33 productivity period, while both *N. incompta* and *G. truncatulinoidea* display a higher
34 calcification during the low productivity period. The comparison of these patterns
35 with environmental parameters revealed that Optimum Growth Conditions
36 temperature and carbonate system parameters are the most likely to influence
37 seasonal calcification in the Gulf of Lions. Interannual analysis suggest that both *G.*
38 *bulloides* and *N. incompta* slightly reduced their calcification between 1994 and



39 2005, while *G. truncatulinoides* exhibited a constant and pronounced increase in its
40 calcification that translated in an increase of 20% of its shell weight for the 400-500
41 μm narrow size class. While our data suggest that carbonate system parameters are
42 the most likely environmental parameter driving foraminifera calcification changes
43 over the years.

44 Finally, comparison between sediment trap data and seabed sediments allowed us
45 to assess the changes of planktic foraminifera calcification during the late Holocene,
46 including the preindustrial era. Several lines of evidence strongly indicate that
47 selective dissolution did not bias the results in any of our data sets. Our results
48 showed a clear calcification reduction between pre-industrial Holocene and recent
49 data with *G. truncatulinoides* experiencing the largest calcification decrease (32-
50 40%) followed by *N. incompta* (20-27%) and *G. bulloides* (18-24%). Overall, our
51 results provide evidence of clear reduction in planktic foraminifera calcification in the
52 Mediterranean most likely associated with ongoing ocean acidification and
53 consistent with previous observations in other settings of the world's oceans.

54

55 **Key words:** Planktic foraminifera, foraminifera calcification, biogeochemical cycles,
56 Ocean Acidification, Mediterranean Sea.

57 1. Introduction

58

59 Growing population and its linked human activity since the industrial period (about
60 170 years ago) has caused an unprecedented rise in carbon dioxide, which
61 ecological and economic consequences are considered a major threat (Ipcc,
62 2022)7/28/22 6:12:00 PM. Atmospheric CO_2 concentrations during the Pleistocene
63 and Holocene ranged from 200 to 280 parts per million (ppm) (Loulergue et al., 2007;
64 Lüthi et al., 2008; Parrenin et al., 2007), but these values have increased dramatically
65 since the onset of the industrial period, exceeding the threshold of 400 ppm in 2015
66 for the first time for at least the last 800.000 years (Lüthi et al., 2008). Between 25
67 and 30% of anthropogenic CO_2 has been absorbed by the world's ocean (Sabine et
68 al., 2004). The ocean uptake of atmospheric CO_2 causes a drop in both pH and
69 carbonate ion concentration (Barker et al., 2012), lowering seawater alkalinity; this
70 process is commonly known as Ocean Acidification (OA), and it is expected to affect
71 all areas of the ocean and to have a wide impact on marine life (Hemleben et al.,
72 1989). One of the main questions about recent environmental change is how
73 different ecosystems and regions in global ocean are going to react to the ongoing
74 increase of anthropogenic atmospheric carbon dioxide.

75 A large body of evidence indicates that ocean acidification has substantial and
76 diverse effects on the distribution and fitness of a wide range of marine organisms



77 (Jonkers et al., 2019; Kroeker et al., 2013; Meier et al., 2014; Moy et al., 2009). For
78 example, some fleshy algae and diatom species have been shown to increase their
79 growth and photosynthetic activity at enhanced CO₂ concentrations (Kroeker et al.,
80 2013). In turn, most calcifying organisms such as calcifying algae, corals, pteropods,
81 coccolithophores and foraminifera are negatively affected by this process often
82 showing a reduction in their abundance, calcification and growth rates (Kroeker et
83 al., 2013; Orr et al., 2005).

84 Planktic foraminifera are a group of marine single-celled protozoans that produce
85 calcareous shells. Their distribution across the water column is conditioned by
86 factors that include, but are not limited to, food availability, temperature, salinity and
87 sunlight (Schiebel and Hemleben, 2005). These organisms are considered to play a
88 key role in marine carbon cycle and carbonate production, accounting for between
89 32 and 80% of the deep ocean calcite fluxes (Schiebel, 2002). Depending on their
90 ecology and feeding strategies, these organisms can be algal (dinoflagellates)
91 symbiont wearing or not symbiont wearing and be spinose or non-spinose. Planktic
92 foraminifera represent a useful tool for palaeoecological and palaeoceanographic
93 studies, as the abundances of different species and their geochemical signature
94 allow reconstructing sea surface temperatures and water column physical and
95 chemical properties (Lirer et al., 2014; Margaritelli, 2020; Schiebel and Hemleben,
96 2017).

97 Previous studies suggest that planktic foraminifera are sensitive to ocean
98 acidification (OA). Laboratory experiments indicate that when carbonate ion
99 concentration decreases, shell weight and calcification decrease too in a variety of
100 species (Bijma et al., 2002; Lombard et al., 2011). Species that host symbionts have
101 been described showing a higher tolerance to dissolution due to the capacity of algal
102 symbionts to alter immediate seawater chemistry (Lombard et al., 2009). Moy et al.
103 (2009) documented a decrease of 30-35% shell weight in the planktic foraminifera
104 *Globigerina bulloides* during the industrial era (defined according to Sabine et al.,
105 2004 from 1800 and therein) in the subantarctic Southern Ocean, most likely induced
106 by anthropogenic-driven ocean acidification. A recent study by Fox et al. (2020)
107 showed that non-spinose (*Neogloboquadrina dutertrei*) foraminifera species exhibit
108 a more pronounced calcification reduction than the spinose (*Globigerinoides ruber*)
109 species in response to increasing CO₂. The main difficulty for studying the impact of
110 OA on foraminifera (and any calcifying organisms) resides in finding long-term
111 continuous records in order to be able to evaluate possible changes in shell
112 calcification (Fox et al., 2020).

113 The Mediterranean Sea is a semi-enclosed sea with a high saturation state for calcite
114 (Álvarez et al., 2014). Moreover, the Mediterranean is also recognized as a sensitive
115 region increasing atmospheric CO₂ (Ziveri, 2012) due to the fast turnover time of its



116 waters (Béthoux et al., 2005) and the fast penetration of anthropogenic CO₂
117 (Schneider et al., 2010). Sea surface temperatures are predicted to increase by 1.5-
118 2°C by the end of the century, a faster rate than the global average (Lazzari et al.,
119 2014). pH is expected to decrease according to the global average (0.3-0.4 units by
120 2100) or even exceed the global trend (Hassoun et al., 2015). The Mediterranean
121 Sea is also affected by other stressors (Durrieu de Madron et al., 2011) which impact
122 marine organisms in many ways (Lejeusne et al., 2009). Finally, it is also a region
123 shaped by human development and its associated activities interact with
124 environmental changes (MedECC).

125 In order to assess the impact of recent environmental change on planktic
126 foraminifera, in this work we present data from Planier sediment trap (data from 1993
127 to 2006) (Rigual-Hernández et al., 2012) and from seabed sediments from three
128 different sites located in both the Gulf of Lions and the promontory of Menorca. The
129 advantage of sediment traps is that they provide data coming from annual fluxes,
130 avoiding the effects of seasonal abundance and ontogeny and making interannual
131 comparisons more reliable (Jonkers et al., 2019). Three different planktic
132 foraminifera species, each of which characterized by contrastingly different depth
133 habitats and ecologies, were selected for our analysis: *Globigerina bulloides*, a
134 spinose opportunist surface dweller that lies above the thermocline (Schiebel and
135 Hemleben, 2014); *Neogloboquadrina incompta*, a non-spinose temperate surface
136 dweller; and *Globorotalia truncatulinoides*, a non-spinose deep dwelling species
137 which migrates through the water column with a complex life cycle. Our aims for this
138 study are: (i) to compare two widely used foraminifera weighing and size-
139 normalization techniques and provide a baseline of modern foraminifera weight data
140 and calcification in the Western Mediterranean against which future changes in
141 foraminifera calcification can be assessed (ii) document seasonal and interannual
142 trends in the planktic foraminifera calcification of the three planktic foraminifera
143 species, and (iii) evaluate possible changes in shell calcification through the
144 Holocene to the present day by comparing shell weights of the foraminifera collected
145 by the traps with those of the seafloor sediments.

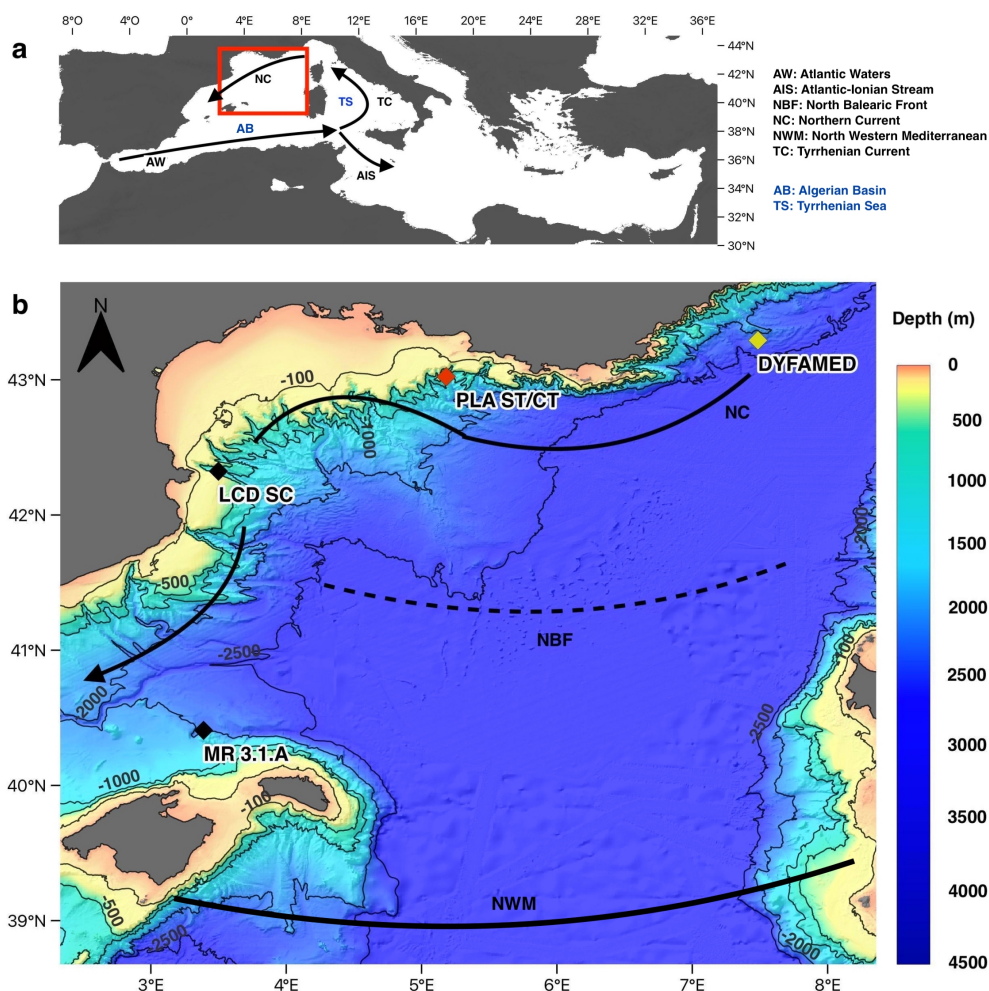
146 2. Study area

147

148 The Mediterranean is a semi-enclosed sea and it is considered a concentration basin
149 (Bethoux et al., 1999) with a negative hydrological budget: fresh water inputs do not
150 compensate the overall basin evaporation. The surface oceanic waters that enter
151 the Mediterranean through the Strait of Gibraltar and spread towards the eastern
152 basin compensate this negative balance. As described by Millot (1999), the thermo-
153 haline properties of the inflowing Atlantic Waters (AW) are gradually modified in their



154 transit towards the Algerian Coast in the form of the Atlantic-Ionian Stream (AIS).
155 The AIS divides into two main branches off the western coast of Sicily: one flows
156 south of Sicily (Béranger et al., 2004) heading towards the Eastern Mediterranean
157 Basin, and the other one enters the Tyrrhenian Sea along the northern coast of
158 Sicily, forming the Tyrrhenian Current (TC) (Figure 1a). The Corsica Channel
159 represents the choke point for water circulation in the Northwestern Mediterranean
160 through which waters of the Tyrrhenian flow into the Ligurian Sea, where the
161 Northern Current (NC) is formed. The NC largely controls the circulation all over the
162 western and northwestern part of the Mediterranean Sea, including the Gulf of Lions
163 and the Balearic Sea (Figure 1a).



164

165

166

Figure 1. a. Study area location in the Mediterranean Sea and general surface circulation **b.** geographic setting of the Gulf of Lions and location of



167 studied sites. Red diamond shows the position of the Planier site sediment
168 trap and core-top (PLA ST/CT). Black diamonds represent the location of the
169 seabed sediments samples analyzed from Lacaze Duthiers canyon (LCD SC)
170 and Menorca promontory (MR 3.1A). Yellow diamond represents the location
171 of the Dynamics of Atmospheric Fluxes in the MEDiterranean Sea
172 (DYFAMED) site, located 200 km upstream Planier station position. Arrows
173 represent the surface circulation (Millot, 1999).

174
175 The Gulf of Lions (GoL) is located in the northwestern part of the Mediterranean Sea,
176 and its morphology presents a continental slope with an array of complex submarine
177 canyons (Rigual-Hernández et al., 2012) (Figure 1b). As previously stated, the
178 general circulation is controlled by the counterclockwise NC flowing along the
179 continental slope (Millot, 1991).
180 Vertical mixing, generated by intense surface cooling and evaporation, occurs in
181 winter in the Gulf of Lions driven by cold, dry northern winds, resulting in dense water
182 on the shelf and offshore (Durrieu de Madron et al., 2005; Houpert et al., 2016; Millot,
183 1991). This winter mixing recharges surface waters with nutrients. This enrichment
184 with increased solar radiation stimulates primary production in spring. Increasing
185 heat fluxes during spring and summer cause water mass stratification and nutrient
186 depletion, which lasts until late summer, until fall cooling breaks the stratification of
187 the water column and causes a fall bloom (Heussner et al., 2006; Monaco et al., 1999;
188 Rigual-Hernández et al., 2012). River inputs are the main source of suspended particles
189 in the Gulf of Lions, and the Rhone river represents the most important river in the
190 northwestern Mediterranean; however, other sources include Saharan dust deposits
191 and biological production (Heussner et al., 2006; Monaco et al., 1999). Overall, the
192 oceanographic setting of the Gulf of Lions is an exception to the general oligotrophy
193 of the Mediterranean Sea.

194 3. Material and methods

195

196 3.1. Sediment traps, core-tops and sediment cores.

197 A series of deployments of sediment traps mooring lines in the Gulf of Lions
198 continental margin was initiated in 1993 within the framework of several French and
199 European projects (PNEC, Euromarge-NB, MTP II-MATER, EUROSTRATAFORM)
200 and the monitoring of two sites, Planier and Lacaze-Duthiers stations (Figure 1),
201 continues as a component of the MOOSE project (Mediterranean Ocean Observing
202 System for the Environment). Planier station (43°02'N, 5°18'E) is located at the
203 northeastern end of the Gulf of Lions, in the axis of the Planier Canyon. The sediment
204 trap used for this work was located at around 530 m water depth in a water column



205 of ~1000 m. Further details of the mooring design can be found in Heussner et al.,
206 2006. The characterization and quantification of planktic foraminifera fluxes for the
207 period 1993 to 2006 were analyzed by Rigual-Hernández et al., 2012. Here, we used
208 the samples from the latter study for our weight and calcification analysis. This
209 sediment trap is used here as a baseline of the planktic foraminifera dwelling in the
210 modern Mediterranean Sea. Moreover, we analyzed a set of core top and sediment
211 cores collected from several locations of the Northwestern Mediterranean that are
212 considered to represent foraminifera assemblages sedimented during the pre-
213 industrial Holocene era (Table 1).

214 **Table 1:** description of the core tops used in this study. Data for PLA CT and
215 LCD SC are available in Heussner et al., (2006), and data concerning MR
216 3.1.A can be found in Cisneros et al., (2016). Conventional ^{14}C ages and 1-
217 sigma uncertainties have been rounded according to convention.

Site	Location	Water depth (m)	Sediment Samples	Dating method	Species	Sample dated	Radiocarbon age (^{14}C years BP)	1-sigma error (^{14}C years)
Planier (PLA CT)	42.989° N 5.121° E	1095	2	^{14}C	<i>Globigerina bulloides</i>	0.5-1 cm	490	60
Lacaze-Duthiers (LCD SC)	42.2656°N 3.54°E	990	7	^{14}C	<i>Globigerina bulloides</i>	0.5-1 cm	460	60
Minorca (MR 3.1.A)	40.29°N 3.37° E	2117	40	^{14}C	<i>Globigerina bulloides</i>	14-14.5 cm	1980	65

218

219 3.2. Sediment core samples processing

220 A total of 2 sediment samples from Planier core top, 7 from Lacaze-Duthiers
221 sediment core and 40 from Minorca sediment core were weighed (Table 1). Dry bulk
222 sediment samples from all sites was weighed using a Sartorius CP124S balance
223 (precision= 0.1mg).

224 The samples were then wet-sieved in order to separate the $<63\mu\text{m}$ fraction and dry
225 sieved to separate the bigger fractions ($>150\mu\text{m}$ and $>300\mu\text{m}$). The sediment
226 washing was carried out with potassium phosphate-buffered solution (pH= 7.5) in
227 order to optimize foraminifera preservation. Each fraction was oven dried at a
228 constant temperature (50°C) and then weighed. The $>150\mu\text{m}$ fraction was used for
229 identification, counting and shell morphometric and weight analyses.

230

231 3.3. Foraminifera picking and mass and size estimations

232 Planktic foraminifera picking focused on three species: *Globigerina bulloides*,
233 *Neogloboquadrina incompta* and *Globorotalia truncatulinoides*. For the latter
234 species, both coiling morphotypes were selected although the right coiling was
235 substantially less abundant representing less than 3% in our counts, a feature



236 consistent with the literature that indicates a low presence of right coiled specimens
237 (Margaritelli et al., 2020; 2022). Different sizes were selected depending on the
238 maximum availability of each species: 250-300, 200-250 and 400-500 μm , for *G.*
239 *bulloides*, *N. incompta* and *G. truncatulinoides*, respectively. A total of 273
240 foraminifera samples were picked for this study, 126 coming from the sediment trap
241 and 147 from the three sediment cores and core tops (Table 2).

242 The mean weight of each available sediment trap sample was obtained by weighting
243 between 15 to 45 specimens of *G. bulloides* (mean $N= 27$), 5 to 25 *N. incompta*
244 (mean $N= 15$) and 5 to 25 *G. truncatulinoides* (mean $N= 13$). Concerning the
245 analyses of the core top and sediment core samples, between 15 and 25 *G. bulloides*
246 and *N. incompta* (mean $N= 20$ for both) and between 9 and 25 *G. truncatulinoides*
247 (mean $N= 18$) were picked.

248 Each foraminifera sample was then cleaned by gentle ultrasonication (50 Hz) for 5
249 to 75 seconds (depending on the species and the degree of visual uncleanliness) in
250 methanol in order to clean the shells. The samples were then left to dry in a
251 temperature-controlled oven at 50°C. One out of three analyzed samples were
252 weighted before and after cleaning in order to assess potential shell mass losses
253 and shell preservation due to ultrasonication. Our results indicate that this method
254 has little impact on shell preservation with around 95% of the total foraminifera
255 conserved in good conditions. Weight loss between non-cleaned samples and
256 cleaned samples are a mean 0.5 to 3 μg depending on the species, mainly due to
257 the presence of clay and non-calcite material in the shells, which justifies this
258 cleaning process.

259 The weightings were carried in the micropaleontology laboratory of the Geology
260 Department at University of Salamanca using a Sartorius ME5 balance (precision=
261 0.001 mg). This method allowed us to obtain foraminifera Sieve Based Weight
262 (SBW) by dividing the average shell weight per sample (5-45 tests) by the total
263 number of foraminifera within each sample.

264 In order to remove the size effect on the weight (Beer et al., 2010) the mean SBW
265 was normalized to the mean diameter and area of the planktic foraminifera to obtain
266 Measurement Based Weights (MBW). Morphometric parameters were measured
267 using a Nikon SMZ18 stereomicroscope equipped with a Nikon DS-Fi3 camera and
268 NISElements software. Foraminifera shells were positioned in order to obtain the
269 maximum area of each individual, in this case, the umbilical side (aperture facing
270 upwards) was measured for the three species.

271 MBW_{area} and $\text{MBW}_{\text{diameter}}$ were calculated according to the following formula
272 (Aldridge et al., 2012; Beer et al., 2010), where “parameter” accounts for “area” or
273 “diameter”:

274



$$275 \quad MBW_{sample} = \frac{mean\ SBW_{sample} \times mean\ parameter_{size\ fraction}}{mean\ parameter_{sample}}$$

276

277 The Area Density (ρA , $\mu g/\mu m^2$) was calculated by dividing the SBW by the mean
278 sample silhouette area (Marshall et al., 2013).

279 Finally, in order to compare weights patterns from the sediment trap with weights
280 from core tops and sediment cores and overcome the seasonality effect, MBWs were
281 flux-weighted. Mean monthly MBWs values from each species were multiplied by
282 the corresponding mean monthly flux and then divided by the total annual flux.

283

284 **3.4. Environmental data**

285 Foraminifera fluxes and abundances together with chlorophyll-*a* were obtained from
286 Rigual-Hernández et al., 2012 for the entire time span of the analyzed samples. Both
287 fluxes and abundance come from direct sediment observation from the Planier site,
288 while chlorophyll-*a* data was obtained from SeaWiFS monthly measurements
289 through NASA's Giovanni program on a 0.2 x 0.2° area around the mooring location.
290 Sea Surface Temperature (SST) was recovered from the NOAA database with the
291 same gridding as the data from the NASA's Giovanni program.

292 Salinity, nutrient concentrations (nitrates and phosphates) and carbonate system
293 parameters data were collected from the DYFAMED database ([http://www.obs-
295 vlf.fr/dyfBase/index.php](http://www.obs-
294 vlf.fr/dyfBase/index.php)). DYFAMED site is located around 200-220km (Figure 1b)
296 east of the sediment trap location (43°25'N, 7°52'E), in the Ligurian Sea. From an
297 oceanographic view, its situation is upstream of the NC circulation and can be
298 considered representative of seasonal and interannual variability of biological and
299 water column properties of the open-ocean waters in the northwestern
300 Mediterranean (Heussner et al., 2006; Meier et al., 2014). Alkalinity and total carbon
301 measurements were available for years 1998 to 2000 and mid 2003 to 2005. Missing
302 values comprised in these years were replaced with values obtained from linear
303 regression of the measurements from above and below. The CO2SYS macro has
304 been used to reconstruct the $[CO_2]$, $[CO_3^{2-}]$, $[HCO_3^-]$ and pH values from the
305 measured total alkalinity and dissolved inorganic carbon. The constants used were
306 the CO_2 dissociation constant by Mehrbach et al., 1973 refit by Dickson and Millero,
307 1987; the $KHSO_4$ by Dickson, 1990; and the seawater scale for pH. In order to have
308 uninterrupted monthly environmental values from the DYFAMED site during
309 available measurements, a resampling every 10 days has been carried out with the
310 QAnalySeries program.

311 Seasonal correlation analyses were carried out with the Statistica program. A $p < 0.05$
312 was used in order to consider a correlation as significant. The number (N) of
313 correlations depended on data availability and was 10 for *G. bulloides*, 9 for *N.*



313 *incompta* and 12 for *G. truncatulinoides*. On an interannual time scale we
314 acknowledge that our data presents some gaps over the years, and some years in
315 the sediment trap and foraminifera record are not well represented, however, trends
316 provided here give a new insight on interannual calcification trends in the
317 northwestern Mediterranean.

318

319 **3.5. Radiocarbon dating**

320 Between 50-100 individuals of well-preserved *Globigerina bulloides* shells (>150
321 μm) were picked for radiocarbon analyses. Radiocarbon ($^{14}\text{C}/^{12}\text{C}$) was measured as
322 CO_2 with a gas ion source in a Mini Carbon Dating System (MICADAS) at the
323 Laboratory of Ion Beam Physics from ETH Zürich. The employed automated method
324 consists of initial leaching of the outer shell to remove surface material with 100 μl
325 of ultrapure HCl (0.02M) and the subsequent acid digestion of the remaining
326 carbonates with 100 μl of ultrapure H_3PO_4 (85%) (Wacker et al., 2013). Therefore,
327 no cleaning was applied after the picking contrary to the samples used for mass and
328 size measurements. Marble (IAEA-C1) was used for blank correction and results
329 were corrected for isotopic fractionation via $^{13}\text{C}/^{12}\text{C}$ isotopic ratios.

330 Both the samples and dates obtained are detailed in Table 1.

331 **4. Results**

332

333 **4.1. Shell morphometric parameters and shell-weight normalization**

334 Table 2 shows the results of the shell area, diameter and SBW, the total foraminifera
335 samples analyzed, the mean number of individuals per sample and the total
336 individuals measured at each of the studied sites.

337 **Table 2.** Minimum, mean, maximum and standard deviation values of shell
338 area, diameter and SBW for *Globigerina bulloides*, *Neogloboquadrina*
339 *incompta* and *Globorotalia truncatulinoides* at all studied sites. The last 3
340 columns show the number of samples, the mean number (N) of individuals
341 analyzed per sample and total number of individuals measured for each site.

342



PLA Sediment Trap	Area (μm^2)				Diameter (μm)				Sieve Based Weight (SBW, μg)				TOTAL	N PER	TOTAL
	Min	Mean	Max	Std.Dev	Min	Mean	Max	Std.Dev	Min	Mean	Max	Std.Dev	SAMPLES	SAMPLE	N
<i>G. bulloides</i>	16978	57353	168492	17261	147.0	267.5	463.2	38.6	3.21	4.43	5.60	0.66	35	27.2	893
<i>N. incompta</i>	26234	42821	135422	8934	182.8	232.4	415.2	22.6	3.17	4.45	5.40	0.59	32	15.0	455
<i>G. truncatulinoides</i>	70712	178952	527622	63572	291.9	468.5	819.6	81.9	10.67	23.11	39.57	7.79	59	13.0	729
PLA Core-Top															
<i>G. bulloides</i>	37163	55395	87894	12302	217.5	264.0	334.5	28.8	5.00	5.22	5.43	0.30	2	17.3	39
<i>N. incompta</i>	27635	36927	49619	5447	187.6	216.3	251.4	15.9	4.46	4.46	4.46	0.00	2	19.7	41
<i>G. truncatulinoides</i>	89778	174748	233229	44313	338.1	467.7	544.9	61.9	34.80	35.40	35.90	0.70	2	14.7	34
MIN Sediment core															
<i>G. bulloides</i>	20895	52132	138424	8722	163.1	256.8	419.8	20.5	4.00	5.07	6.57	0.46	40	19.6	761
<i>N. incompta</i>	24003	35098	57264	4658	174.8	211.0	270.0	13.7	3.45	4.11	5.00	0.34	40	20.3	791
<i>G. truncatulinoides</i>	116686	166318	365851	23262	385.4	459.1	682.5	30.8	28.33	34.99	42.60	3.25	40	14.4	576
LCD Sediment core															
<i>G. bulloides</i>	27624	52472	116605	8793	187.5	257.7	385.3	20.4	4.35	4.73	5.19	0.31	7	20.1	136
<i>N. incompta</i>	28089	37789	51284	4972	189.1	218.9	255.5	14.4	3.68	4.12	4.50	0.26	7	19.8	134
<i>G. truncatulinoides</i>	82534	143138	393754	41620	324.2	423.3	708.1	55.9	25.27	26.68	30.66	1.94	7	15.3	105

343

344

345 Overall, the mean values for both diameter and area correspond to mean narrowed
 346 size fraction used during the picking, but morphometric parameters show some
 347 variability between the studied sites. Standard deviation of both area and diameter
 348 values for the three species are higher in the sediment trap record than in seafloor
 349 sediments, with mean values (of all three species) of 82% higher for area and 69%
 350 higher for diameter. SBW exhibits the same pattern as both area and diameter
 351 standard deviation is a mean 130% higher in the Planier sediment trap. Regarding
 352 the variability across the seafloor samples, Planier core-top exhibits a greater area
 353 and diameter values (about 40 to 50% increase for the three species) compared to
 354 those of the other two sediment cores, probably due to the fewer samples analyzed
 355 (Table 2).

356 The Planier sediment trap results (Table 2) show a higher standard deviation for both
 357 area and diameter for the three species, i.e. 76 % and 68% higher for *G. bulloides*
 358 compared to the data from core tops, 78% and 54% for *N. incompta* and 81% and
 359 73% for *G. truncatulinoides*.

360 Because of the lack of precision of the initial individuals picking, carried out with a
 361 micrometer installed in the microscope, the selection is not totally accurate. Due to
 362 this issue, one third of the of the total measured foraminifera (i.e. 1645 of 4694) were
 363 out of the desired size fraction, of which 12% were bigger (580/4694) and 23% were
 364 smaller (1065/4694). Nonetheless, only 0.02% were more than 20% out of the
 365 selected size range (64/4694 more than 20% bigger and 29/4694 more than 20%
 366 smaller). Mean size difference for the foraminifera out of the size fraction is around
 367 7%. Results vary according to the site and the species. 50% of the individuals from

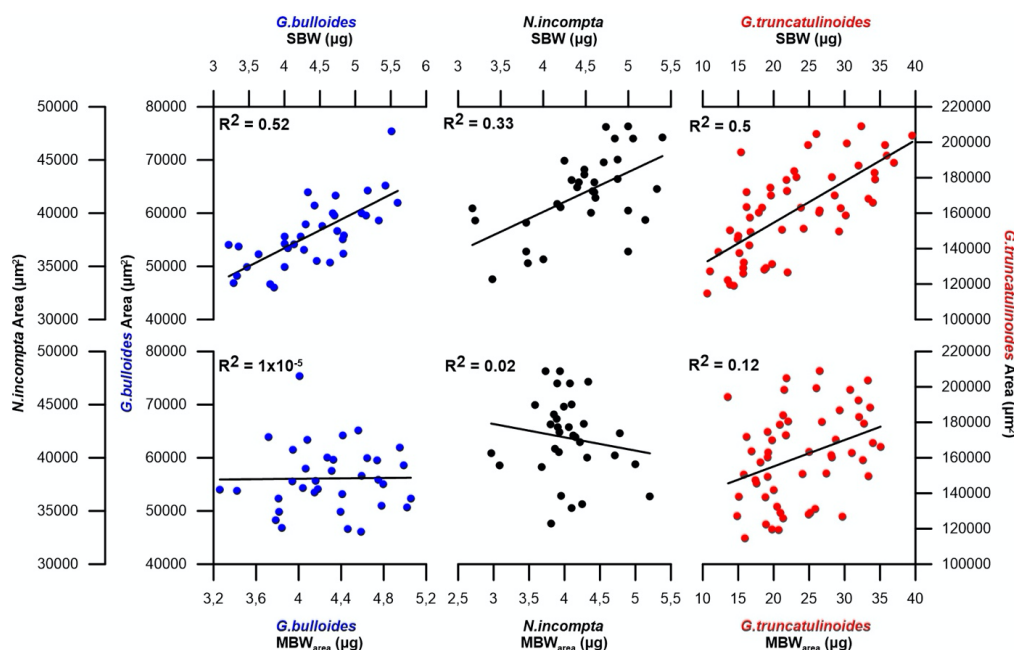


368 the Planier sediment trap (1046/2077) and 26% of the individuals coming from the
 369 core tops (692/2617) were out of range. *G. bulloides* showed a 45.5% (53.2% in the
 370 sediment trap and 39.3% in the core-tops samples) of individuals out of selected size
 371 fraction, while this value is 21.5% (22.2% in sediment trap, 21.1% in sediment cores)
 372 for *N. incompta* and 35% for *G. truncatulinoides* (53.4% in sediment trap, 16.7% in
 373 sediment cores).

374

375 Even though a narrow size class was selected for each species (See section 3.3), a
 376 clear correlation between area and SBW was found in our data set (Figure 3).

377



378

379 **Figure 2.** SBW in µg and MBW_{area} in µg against the mean test area in µm² for
 380 foraminifera samples in the Planier sediment trap. Dark blue dots correspond
 381 to *G. bulloides*, black dots to *N. incompta* and red dots to *G. truncatulinoides*.

382 In Figure 2, we show the values for the Planier sediment trap record for both SBW
 383 and MBW_{area} for all three species considered in this study, and their correlation with
 384 the measured area. In particular, SBW shows a positive correlation with area:
 385 $0.33 < r^2 < 0.53$. This indicates that the SBW is dependent on the size of the specimens
 386 within the selected size range. Thus, to isolate the component of variation in
 387 foraminifera shell thickness that represents a change in calcification and does not
 388 occur as a direct result of changes in shell size, normalization of the shell weight was
 389 performed following the formula detailed in section 3.3. (Beer et al., 2010). After



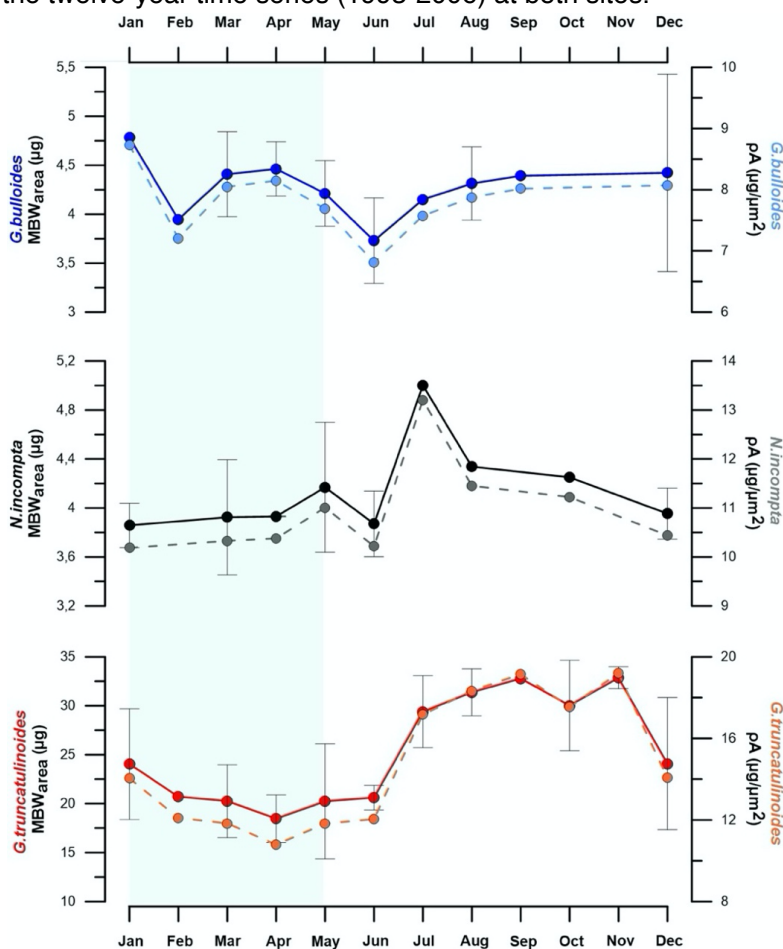
390 normalization MBW_{area} shows no correlations with area: $1 \times 10^{-5} < r^2 < 0.12$ (Figure 2).
391 Note that the weight variations in our dataset are quite considerable, especially for
392 *G. truncatulinoides*, probably due to the wider size fraction. Diameter does show
393 correlation with SBW: $0.33 < r^2 < 0.5$; and shows a non-negligible correlation with
394 MBW_{diam} : $0.2 < r^2 < 0.33$. Our data demonstrates that SBW correlates more strongly
395 with MBW_{diam} than with MBW_{area} for the 3 species: $0.9 > 0.48$ for *G. bulloides*,
396 $0.89 > 0.52$ for *N. incompta* and $0.97 > 0.81$ for *G. truncatulinoides*. These values are
397 consistent with previous studies (Beer et al., 2010).
398 Differences between SBW and both MBW_{area} and MBW_{diam} vary depending on the
399 species: SBW is slightly heavier for *G. bulloides*, heavier for *N. incompta* and lighter
400 for *G. truncatulinoides*. The mean standard deviation for all 3 species is around 8%:
401 7.8% for *G. bulloides*, 6.4% for *N. incompta* and 13% for *G. truncatulinoides*. We
402 take these values as the error adjustment for SBW in the different size fractions (250-
403 300 μm , 200-250 μm and 400-500 μm respectively). It is difficult to compare these
404 results with other studies as size fractions and species are often different, but this
405 error estimates are in the same order of magnitude as some other MBW published
406 in core-tops records and sediment traps (de Moel et al., 2009; Moy et al., 2009).
407 These findings highlight the fact that the use of sieve fractions does not provide
408 enough control on the influence of morphometric parameters in test weight.
409 Morphometric variations described in table 1 indicate that the typically used sieve
410 fractions may be unreliable due to the number of individuals out of the desired
411 fractions. The correlations between SBW and shell area are consistent with previous
412 studies (Aldridge et al., 2012; Beer et al., 2010) and underscore the importance of
413 isolating the component of variation in foraminifera shell thickness that represents a
414 change in calcification and does not occur as a direct result of change in shell size.
415 Thus, the shell weight was size-normalized after Beer et al., 2010 by isolating the
416 influence of isometric scaling on wall thickness and calcification density.
417 Area and diameter show a perfect correlation ($r^2 = 1$) for all 3 species, highlighting a
418 relationship between the different MBWs. Moreover, both MBW_{area} (Figure 2) and
419 MBW_{diam} , in either the sediment trap data and core-top data, do not correlate with
420 area and diameter ($1 \times 10^{-5} < r^2 < 0.33$ and $0.001 < r^2 < 0.2$ respectively) indicating that
421 size does not have an influence on these values. This suggests that our size-
422 normalization procedure adequately removes the size influence and therefore, our
423 MBW data represents a robust parameter reflecting test wall thickness and
424 calcification intensity not influenced by test size. Therefore, MBWs can be
425 considered as a reliable calcification intensity proxy.
426 Based on all the above, from this point we'll focus our discussion on the MBW_{area}
427 and ρA (area density) to discuss the foraminifera shell weight variability on seasonal,
428 interannual and pre-industrial Holocene time scales.



429

430 **4.2. Seasonal variations of foraminifera calcification in the NW Mediterranean**

431 Mean annual MBW_{area} and ρA values were calculated for the three species to
 432 illustrate the seasonal variability of these parameters (Figure 3). Monthly data
 433 corresponds to the average result of all the data corresponding to each month
 434 between the twelve-year time series (1993-2006) at both sites.



435

436 **Figure 3.** Mean MBW_{area} and ρA ($\times 10^{-5}$) composite year values for *G.*
 437 *bulloides* (dark and light blue lines), *N. incompta* (black and grey lines) and
 438 *G. truncatulinooides* (red and orange lines) in the Planier sediment trap across
 439 a composite year. Light green back represents the high productivity period in
 440 the study zone (Rigual-Hernández et al., 2012).

441 The mean MBW_{area} and ρA for the three species in the Planier sediment trap are
 442 $4.29 \mu g$ ($\pm 0.45 \mu g$) and 7.81 (± 0.91), respectively, for *G. bulloides*, 4.04 ($\pm 0.4 \mu g$)



443 μg and $10.67 (\pm 1.21)$ for *N. incompta* and $23.25 (\pm 6.2 \mu\text{g})$ μg and $13.57 (\pm 3.6)$ for
444 *G. truncatulinoides*.

445 The temporal variations in shell calcification exhibit a clear seasonal pattern for the
446 three species. The composite year shows that all the three species exhibit a clear
447 but different seasonal pattern (Figure 3).

448 In the case of *G. bulloides*, maximum annual calcification values are reached during
449 winter (January; $4.78 \mu\text{g}$), and minimum during summer (June; $3.72 \mu\text{g}$). The
450 observed $1 \mu\text{g}$ difference in calcification between maximum and minimum values
451 corresponds to a 24.5% change in the mean MBW_{area} value. Mean seasonal
452 standard deviation is $\pm 0.47 \mu\text{g}$, with the lowest value in April, $\pm 0.27 \mu\text{g}$; and the
453 highest value in December, $\pm 1 \mu\text{g}$.

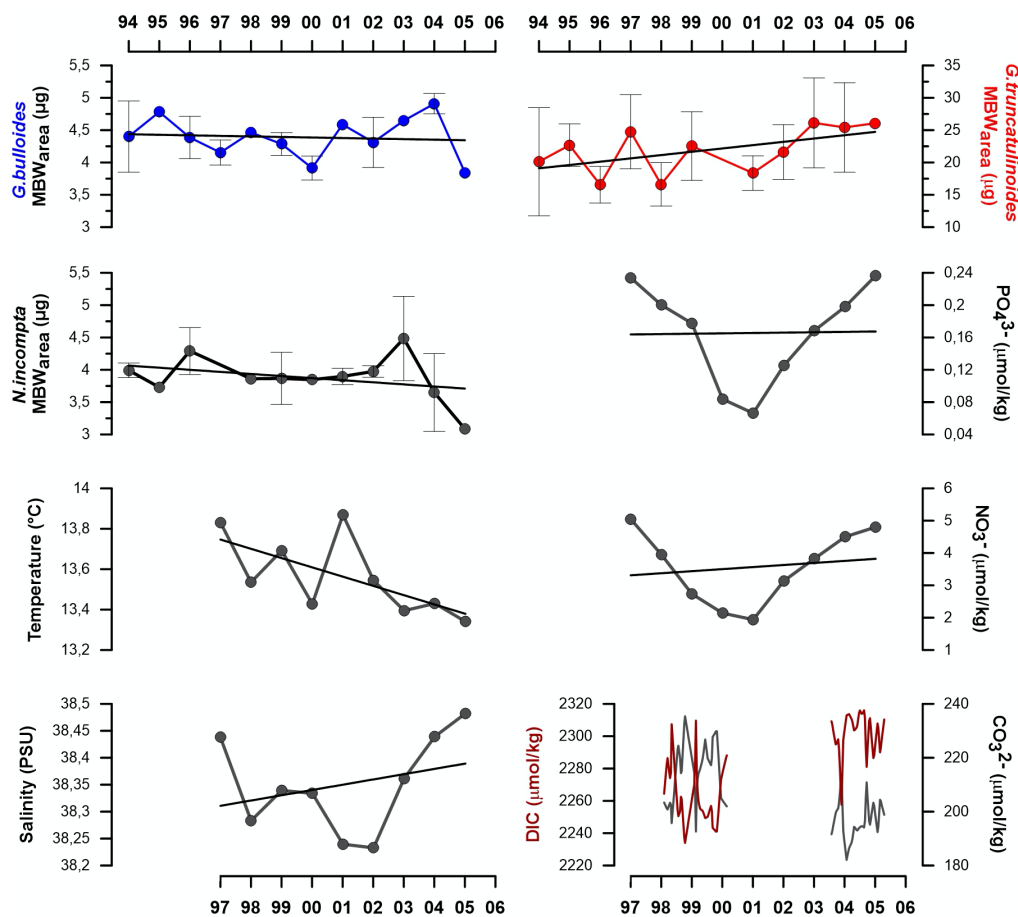
454 *Neogloboquadrina incompta* shows a maximum in calcification in mid-summer (July;
455 $5 \mu\text{g}$) and two minima in mid-winter (January; $3.85 \mu\text{g}$) and early summer (June; 3.87
456 μg). Thus, the annual seasonal amplitude is $1.15 \mu\text{g}$ which translates into a 28%
457 seasonal MBW_{area} variability. Standard deviation is $\pm 0.28 \mu\text{g}$, with the highest value
458 in May, $\pm 0.53 \mu\text{g}$; and the lowest one in April with no deviation.

459 Finally, *G. truncatulinoides* displays a seasonal maximum MBW_{area} value in late
460 summer- autumn (November; $32.85 \mu\text{g}$) and minima in spring (April; $18.45 \mu\text{g}$).
461 Seasonal MBW_{area} difference is $14.3 \mu\text{g}$: a 60% variability. Mean typical seasonal
462 deviation is $\pm 3.7 \mu\text{g}$, with December and November showing the highest and lowest
463 variability respectively: ± 1.1 and $\pm 6.7 \mu\text{g}$.

464

465 **4.3. Interannual MBW_{area} trend**

466 Trends throughout the record are represented in Fig 4. In order to obtain
467 representative data for each year, maximize data availability of each species and
468 avoid the impact of non-representative months on the interannual trends, only MBWs
469 from the productive period (January to May) of each year analyzed were included.
470 The same strategy was applied for the environmental data, with the exception of the
471 carbonate system parameters.



472

473 **Figure 4.** Inter-annual variations in the *G. bulloides*, *N. incompta* and *G.*
 474 *truncatulinoides* MBW_{area} and the environmental data from the DYFAMED site
 475 (available since 1997). Except for the carbonate system parameters, trends
 476 represent mean values from the high productivity period of each year (see
 477 study area). DIC represents Dissolved Inorganic Carbon. Black lines
 478 represent the trends from the MBW_{area} and resampled data.

479 Planktic foraminifera calcification variability across the twelve-year record varied
 480 depending on the species (Figure 4). *G. bulloides* MBW_{area} showed a slight but
 481 constant decrease over the studied interval. Minimum values were reached during
 482 years 2000 and 2005 (3.9 and 3.85 µg respectively). On the other hand, *N. incompta*
 483 MBW_{area} showed little to none interannual variability, excepting a calcification
 484 reduction the last two years (3.1 µg). Finally, *G. truncatulinoides* MBW_{area} showed a
 485 different pattern, with a constant and steep calcification increase throughout the



486 record, with minimum calcification values observed in 1996 (16.5 μg) and maximum
487 in 2003 (26.1 μg).

488 Temperature (SST) displayed a constant decrease over the years, from 13.8 to 13.4
489 $^{\circ}\text{C}$, while salinity showed a slight increase, mainly since 2002. From late 2000 until
490 late 2002, nutrient concentrations were exceptionally low (Figure 4). This feature has
491 already been described in the Gulf of Lions (Meier et al., 2014). However, data from
492 the carbonate system showed variations across the years. Between the 2 periods
493 for which direct on-situ measurements were available, 1998 to 2000 and 2003 to
494 2005 (Figure 4) CO_3^{2-} dropped by 10-15 $\mu\text{mol}/\text{kg}$, DIC increased by 40 to 60 $\mu\text{mol}/\text{kg}$,
495 leading to a pH decrease of 0.02 to 0.025. Meier et al., 2014, linked this pH decrease
496 to recent years coccoliths weight reductions in the Gulf of Lion.

497

498 **4.4. Sediment trap, core tops and sediment cores MBW patterns**

499 Foraminifera weights analyzed in core tops and sediment cores from the NW part of
500 the Mediterranean allowed a further insight on the reduced foraminifera calcification
501 during the Holocene (Figure 6).

502 Flux weighted MBWs (see section 3.3) from Planier sediment trap for the three
503 planktic species were 4.1 μg for *G. bulloides*, 3.3 μg for *N. incompta* and 22.3 μg for
504 *G. truncatulinoides* (Figure 6). Data from Planier core-top showed higher mean
505 MBW_{area} values: 5.3 μg , 4.65 μg and 35.4 μg . ^{14}C dating in this core-top revealed a
506 date of 489 years (± 59 years). Overall, in the last 489 years, *G. bulloides* weight has
507 been reduced by 1.2 μg , *N. incompta* by 1.3 μg and *G. truncatulinoides* by 12-13 μg .
508 Located west of Planier site, Lacaze Duthiers sediment core mean MBWs were:
509 4.99 μg for *G. bulloides*, 4.14 μg for *N. incompta*, and 32.9 μg for *G. truncatulinoides*.
510 ^{14}C dating was carried out on the core-top sample of this sediment core that
511 displayed a date of 460 years (± 59 years). Corresponding MBWs from this sample
512 for *G. bulloides*, *N. incompta* and *G. truncatulinoides* respectively were: 4.7 μg ,
513 4.2 μg and 34 μg . Overall, compared to the data from the sediment trap, this
514 corresponds to a 0.6 μg weight loss for *G. bulloides*, 0.9 μg for *N. incompta* and 12.2
515 μg for *G. truncatulinoides* in 460 years.

516 Located in the Gulf of Minorca, northwest of Planier site, Minorca sediment core
517 mean MBWs were: 5.4 μg for *G. bulloides*, 4.5 μg for *N. incompta* and 36.3 μg for
518 *G. truncatulinoides* (Figure 6). ^{14}C dating on this core top was carried out on an
519 intermediate depth (see section 3.4) due to the lack of availability of enough
520 specimens in the core-top and displayed a date of 1979 years (± 63 years).
521 Corresponding MBWs for this sample were 4.9 μg , 4.4 μg , 35.1 μg for the three
522 species. Therefore, weight reduction was: 0.8 μg for *G. bulloides*, 1.1 μg for *N.*
523 *incompta* and finally, 12.8 μg for *G. truncatulinoides*.



524 5. Discussion

525

526 **5.1. Seasonal controls on planktic foraminifera shell calcification in the NW**
 527 **Mediterranean**

528 As described in section 4.2., the seasonal variability of MBW_{area} displays important
 529 differences across the three species analyzed. The different seasonal pattern in
 530 MBW_{area} is reflected by the lack of correlation between the seasonal pattern of
 531 MBW_{area} of the different species, i.e., $r = -0.23$ ($p > 0.05$) between *G. bulloides* and *N.*
 532 *incompta* and $r = 0.16$ ($p > 0.05$) between *G. bulloides* and *G. truncatulinoides*. Only
 533 the seasonality of *N. incompta* MBW_{area} and *G. truncatulinoides* MBW_{area} share some
 534 similarities, as reflected in the significant and positive correlation ($r = 0.66$; $p < 0.05$).
 535 In order to examine the main controls on foraminifera seasonal calcification in the
 536 Gulf of Lions, here we compare the seasonal variability of planktic foraminifera
 537 calcification with foraminifera fluxes previously estimated for the Planier sediment
 538 trap (Rigual-Hernández et al., 2012), satellite data for the studied site and a suite of
 539 environmental parameters measured at the DYFAMED site (see section 3.4).

540 **Table 3.** Correlation matrix of seasonal test weights and the environmental
 541 parameters from Planier (sediment trap and satellite data) and DYFAMED
 542 site (see section 3.4). Significant correlations ($p < 0.05$) are set in bold.

Parameters	Planier site data						DYFAMED site data							
	<i>G. bull.</i>	<i>N. inc.</i>	<i>G. truncat.</i>	<i>G. bull.</i>	<i>N. inc.</i>	<i>G. truncat.</i>	Chl-a	SST	Salinity	[NO ₃]	[PO ₄]	pH	[CO ₃]	[CO ₂]
	MBW _{area}			Fluxes										
Planier site data	<i>G. bull.</i>	-0.232	0.167	0.012	0.027	0.152	0.318	-0.320	-0.163	0.292	0.330	0.096	-0.189	0.243
	<i>N. inc.</i>	-0.232	0.667	-0.582	-0.407	-0.405	-0.484	0.688	0.368	-0.272	-0.235	-0.350	0.474	-0.280
	<i>G. truncat.</i>	0.167	0.667	-0.905	-0.725	-0.666	-0.585	0.672	-0.299	-0.258	-0.512	-0.113	0.732	-0.541
	<i>G. bull.</i>	0.012	-0.582	-0.905	0.911	0.861	0.773	-0.755	0.264	0.338	0.526	0.213	-0.748	0.548
	<i>N. inc.</i>	0.027	-0.407	-0.725	0.911	0.953	0.817	-0.621	0.364	0.329	0.391	0.103	-0.700	0.596
	<i>G. truncat.</i>	0.152	-0.405	-0.666	0.861	0.953	0.739	-0.707	0.446	0.586	0.590	-0.012	-0.801	0.714
Chl-a	0.318	-0.484	-0.585	0.773	0.817	0.739	-0.702	-0.004	0.190	0.277	0.501	-0.428	0.255	
SST	-0.320	0.688	0.672	-0.755	-0.621	-0.707	-0.702	0.047	-0.688	-0.696	-0.416	0.649	-0.410	
Salinity	-0.163	0.368	-0.299	0.264	0.364	0.446	-0.004	0.047	0.305	0.420	-0.714	-0.604	0.733	
DYFAMED site data	[NO ₃]	0.292	-0.272	-0.258	0.338	0.329	0.586	0.190	-0.688	0.305	0.876	-0.183	-0.682	0.620
	[PO ₄]	0.330	-0.235	-0.512	0.526	0.391	0.590	0.277	-0.696	0.420	0.876	-0.162	-0.834	0.709
	pH	0.096	-0.350	-0.113	0.213	0.103	-0.012	0.501	-0.416	-0.714	-0.183	-0.162	0.338	-0.596
	[CO ₃]	-0.189	0.474	0.732	-0.748	-0.700	-0.801	-0.428	0.649	-0.604	-0.682	-0.834	0.338	-0.939
	[CO ₂]	0.243	-0.280	-0.541	0.548	0.596	0.714	0.255	-0.410	0.733	0.620	0.709	-0.596	-0.939

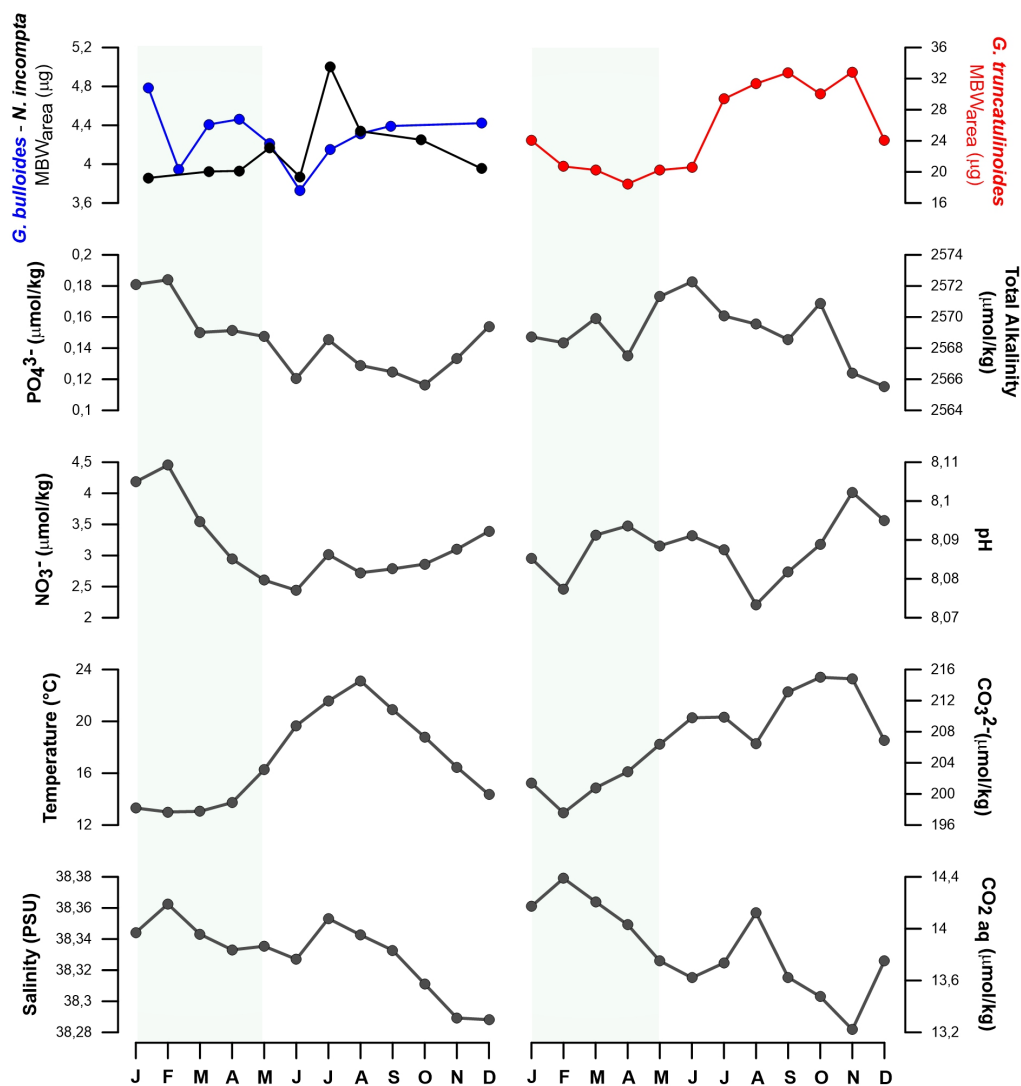
543

544 Among all the environmental parameters, de Villiers (2004) suggested that shell
 545 calcification, and therefore MBWs, is primarily controlled by the Optimum Growth
 546 Conditions (OGC) that can be defined as the most suitable environmental conditions
 547 for the development of a given planktic foraminifera species. Based on the latter



548 study, it could be expected that favorable environmental conditions for foraminifera
549 growth would lead to both greater shell fluxes and enhanced shell calcification. Our
550 correlation analysis shows different relationships between foraminifera abundance
551 (as inferred from foraminifera shell fluxes) and shell weight. In particular, *G. bulloides*
552 MBW_{area} shows no correlation with its fluxes (Table 3), while both *N. incompta* and
553 *G. truncatulinoides* exhibit a negative correlation between MBW_{area} and their species
554 fluxes although only significant for the latter species ($r = -0.4$, $p > 0.05$ and -0.66 ,
555 $p < 0.05$ respectively). Interestingly, *G. truncatulinoides* calcification correlates
556 negatively and significantly with all three species fluxes, a pattern opposite to what
557 the OGC theory predicts (de Villiers, 2004), i.e., optimum ecological niche is
558 associated with enhanced calcification. Thus, a possible explanation reconciling our
559 observations with the OGC theory may be that *G. truncatulinoides* tend to prioritize
560 energy allocation toward growth and reproduction at the price of a reduced
561 calcification.

562 An alternative proxy for OGC that may be considered is chlorophyll-*a* concentration.
563 Chlorophyll is considered an indicator of the algal biomass concentration, which is
564 known to represent a large part of some foraminifera species diet, specially for *G.*
565 *bulloides* (Schiebel and Hemleben, 2017). Our data shows a positive but not
566 significant correlation between chlorophyll concentration and *G. bulloides* MBW ($r =$
567 0.32 , $p > 0.05$), suggesting a negligible influence of phytoplankton concentration on
568 *G. bulloides* calcification. A stronger trend would be expected under the OGC theory
569 as algae are a vital part of its diet (Hemleben et al., 1989). We speculate that *G.*
570 *bulloides* may feed only on certain groups of phytoplankton which changes in
571 seasonal abundance in the photic zone do not necessarily follow the seasonal
572 pattern of total chlorophyll concentration (Marty et al., 2002). In the case of *N.*
573 *incompta* and *G. truncatulinoides*, correlations between MBW_{area} and chlorophyll-*a*
574 are negative and stronger although only significant for the latter species ($r = -0.58$,
575 $p < 0.05$). This observation indicates that optimum calcification conditions for *G.*
576 *truncatulinoides* are reached at times of minimum annual algal biomass
577 concentration in the photic zone. It is possible that, due to its deeper habitat
578 (Schiebel and Hemleben, 2017), *G. truncatulinoides* feeds on phytoplankton
579 dwelling in subsurface levels of the water column. In fact, a deep chlorophyll
580 maximum is known to develop during large part of the year in the Northwestern
581 Mediterranean (Estrada et al., 1993) but its presence is not detected by satellites.
582 This interpretation is in agreement with earlier work by Pujol and Vergnaud Grazzini
583 (1995) who found peak abundances of this species during the summer below the
584 thermocline.



585

586

587

588

589

Figure 5. *Globigerina bulloides*, *Neogloboquadrina incompta* and *Globorotalia truncatulinoides* seasonal MBW_{area} variations compared with resampled seasonal signal of environmental parameters from the DYFAMED site across a composite year.

590

591

592

593

594

595

Something to consider when using chlorophyll as an OGC proxy is that it can be confounded with the nutrient concentrations. Previous studies have described that, in those settings where foraminifera abundance covaries with nutrient concentrations, then nutrients are probably a better OGC proxy than chlorophyll concentrations (Schiebel et al., 2001). In turn, the correlation of nutrients (nitrates and phosphates) with fluxes were positive for all three species, although only



596 significant ($p < 0.05$) for *G. truncatulinoides* abundance ($r = 0.58$ and 0.59 for nitrates
597 and phosphates respectively).

598 It is important to note that nitrate and phosphate concentration variations were
599 closely linked to each other ($r = 0.876$, $p < 0.05$) (Table 3), making it difficult to
600 determine if the resulting effect on foraminifera calcification is due to the effect of a
601 single driver or to the combination of both. High phosphate concentrations are
602 generally considered an inhibitor for foraminifera calcification (Zeppenfeld, 2019).
603 Evidences show that calcite formation is inhibited by PO_4^{3-} due to its adsorption on
604 the calcite surface, impeding its precipitation by blocking the crystal growth. Aldridge
605 et al., 2012 showed a negative effect of phosphate concentration on *G. bulloides*
606 and this feature has been shown in other calcareous organisms such as
607 coccolithophores (Paasche and Brubank, 1994) and calcifying algae (Demes et al.,
608 2009), resulting in a higher growth and calcification under controlled PO_4^{3-} . On the
609 other hand, no studies show a reduced calcification in marine organisms under high
610 NO_3^- values. Our work shows that nutrient concentrations (both nitrates and
611 phosphates) do not correlate significantly with any of the three species MBW studied.
612 NO_3^- correlations were not significant for all three species, while PO_4^{3-} correlations
613 were also very weak, with the exception of the one with *G. truncatulinoides* MBW_{area}
614 ($r = -0.512$, $p = 0.07$) (Table 3). Although the p-value of this correlation is slightly
615 higher than what we use as threshold for significance (i.e., 0.05), the negative
616 correlation between *G. truncatulinoides* MBW_{area} and phosphate could be
617 considered almost significant. Thus, our data suggest that enhanced $[\text{PO}_4^{3-}]$ levels
618 could act as an inhibitor for *G. truncatulinoides* calcification in our study region.

619 Previous studies have suggested that salinity may have an influence on foraminifera
620 calcification. Zarkogiannis et al., (2022) found that salinity may control calcification
621 of certain foraminifera species in the central Atlantic region. However, our data
622 suggest that the role of salinity on calcification in our study region is unlikely since
623 its seasonal amplitude is tiny (0.1 PSU; Figure 6). This idea is supported by the lack
624 of correlation between salinity and MBW_{area} for the three species studied (Table 3).
625 Temperature (Sea Surface Temperature) has been described as a major factor that
626 controls the size (Schmidt et al., 2004) and porosity (Burke et al., 2018) of planktic
627 foraminifera, therefore it could represent a major control factor on shell calcification
628 in the NW Mediterranean. In particular, calcification could be positively linked to
629 temperature through different mechanisms: (i) warmer temperatures have been
630 shown to increase enzymatic activity and therefore enhanced growth and
631 calcification rates (Spero et al., 1991); (ii) Lombard et al., (2011) stated that higher
632 temperatures could also increase feeding and ingestion rates, but it remains unclear
633 if this could result in a calcification rate increase. Our data revealed that SST
634 correlates negatively, but without significance with *G. bulloides* calcification, while



635 correlations between SST and *N. incompta* and *G. truncatulinoides* were both
636 positive and significant ($r= 0.69$ and 0.67 respectively, $p<0.05$). These trends could
637 be expected considering the relationship between temperature and nutrient
638 concentrations ($r= -0.69$ and -0.70 for NO_3^- and PO_4^{3-} respectively) and the
639 correlations between the three species MBW_{area} and nutrients concentrations
640 (Figure 5). Finally, in addition to having an impact on the size and calcification of the
641 planktic foraminifera, temperature is well known as a major control of the carbonate
642 system, due to the increased solubility of atmospheric CO_2 at lower temperatures,
643 and therefore it could have an indirect effect on foraminifera calcification by affecting
644 the carbonate system.

645 Data for the carbonate system were only available for years 1998 to 2000 and 2003
646 to 2005 and, therefore gaps comprised in these years were filled with estimates
647 using the CO2sys macro (see Methods). The relationship between CO_3^{2-} and MBW
648 has been described in previous studies (Barker and Elderfield, 2002; Marshall et al.,
649 2013) and the bulk of evidence indicates that foraminifera MBWs to be positively
650 linked with CO_3^{2-} concentrations (Aldridge et al., 2012; Osborne et al., 2016).
651 However, it appeared that planktic foraminifera response to CO_3^{2-} was not uniform
652 and varied across species (Beer et al., 2010; Lombard et al., 2010). The trends
653 between carbonate system parameters and MBWs were similar to those observed
654 when comparing MBWs with temperature, highlighting the covariations between
655 these two parameters (Figure 5). Our data showed that CO_3^{2-} concentrations were
656 not significantly correlated with *G. bulloides* MBW_{area} nor with *N. incompta*. Only *G.*
657 *truncatulinoides* MBW_{area} displayed a clear significant correlation with CO_3^{2-}
658 concentration ($r= 0.73$, $p<0.05$), implying that carbonate availability may represent a
659 key control on *G. truncatulinoides* in the Northwestern Mediterranean. On the other
660 hand, CO_2 concentrations, excepting a negative and almost significant relationship
661 with *G. truncatulinoides* MBW_{area} ($r= -0.54$, $p= 0.06$), showed no correlation with the
662 other 2 species MBWs. None of the remaining carbonate system parameters (pH,
663 alkalinity and calcite saturation), exhibited a significant seasonal correlation with the
664 MBWs.

665 In summary, OGC, SST and CO_3^{2-} are the most likely parameters that control the
666 seasonal changes in the planktic foraminifera species studied here. The combined
667 effect of these parameters seems to control foraminifera calcification in the Gulf of
668 Lions; however, it should be considered that covariation between these parameters
669 is strong, and therefore it is difficult to isolate the effect of a single parameter. Our
670 results are in agreement with earlier studies that stated that OGC (de Villiers, 2004),
671 temperatures and CO_3^{2-} (de Villiers, 2004; Marshall et al., 2013; Osborne et al.,
672 2016) concentrations are the main factors that impact calcification in planktic
673 foraminifera.



674

675 **5.2. Interannual trends in planktic foraminifera calcification**

676 As stated previously, the Mediterranean Sea is a sensitive zone to atmospheric CO₂
677 accumulation (Ziveri, 2012) and is experiencing ongoing ocean acidification. On an
678 interannual time scale, different studies (Beer et al., 2010; Osborne et al., 2016)
679 have shown that sea surface warming and carbonate system parameters are the
680 most likely parameters to control calcification on key calcifying phytoplankton
681 species such as the coccolithophore *Emiliana huxleyi* organisms (Meier et al.,
682 2014). However, datasets from sediment traps that cover a wide span of years and
683 in which foraminifera weights have been analyzed are rare (Kiss et al., 2021),
684 therefore it is difficult to place our results in a more global context. Our analysis
685 suggests that the trends observed in the carbonate system (Figure 5), i.e., the DIC
686 rise and [CO₃²⁻] decrease may be responsible for the slight calcification reduction in
687 both *G. bulloides* and *N. incompta*, particularly in recent years. During the second
688 time span carbonate parameters were available (2003 to 2005), both of these
689 species started experiencing a calcification reduction (Figure 5). *G. bulloides*
690 displayed a relative maximum MBW_{area} in 2004, corresponding to a relative
691 maximum in [CO₃²⁻] and relative minimum in DIC. While in 2005, calcification started
692 to decrease, according to the opposite pattern in [CO₃²⁻] and [CO₂]. *N. incompta*
693 started a decreasing calcification pattern from 2003 to 2005, matching the carbonate
694 system parameters trends in recent years. Our data showed that pH decreased from
695 a mean 8.12 for the 1998-2000 years to a mean 8.08 for the 2003-2005 years. This
696 pH decrease, combined with the carbonate system parameters seem to affect *G.*
697 *bulloides* and *N. incompta* calcification patterns in recent years, however, the degree
698 to which each species react to a change in these parameters differs.

699 Notably, the trend in *G. truncatulinoides* is opposed to the previous two species and
700 shows a steady and steep increase throughout our record. Over the analyzed time
701 span, its MBW increased around 20% (equivalent to an increase of ~5 µg). If this
702 calcification increase continues on current trends, then the average MBW of *G.*
703 *truncatulinoides* will double by 2024. Analysis of present *G. truncatulinoides*
704 populations is urgently needed to assess if the observed trend held true during the
705 last two decades. It is important to note that while *G. truncatulinoides* exhibits an
706 intimate correlation with [CO₃²⁻] on a seasonal scale, no clear correlation was found
707 with the interannual changes of [CO₃²⁻] (Figure 5). In fact, our analysis suggests that
708 the most likely environmental parameter exerting an influence on the calcification of
709 this species is nitrate concentration (Figure 5). A similar enhancement in shell
710 calcification has been described in the Balearic Sea for *G. truncatulinoides* in high-
711 resolution sediment cores (Pallacks et al., 2020), but also in *Globorotalia inflata*.
712 Taken together, our observations and the study mentioned above, suggest that deep

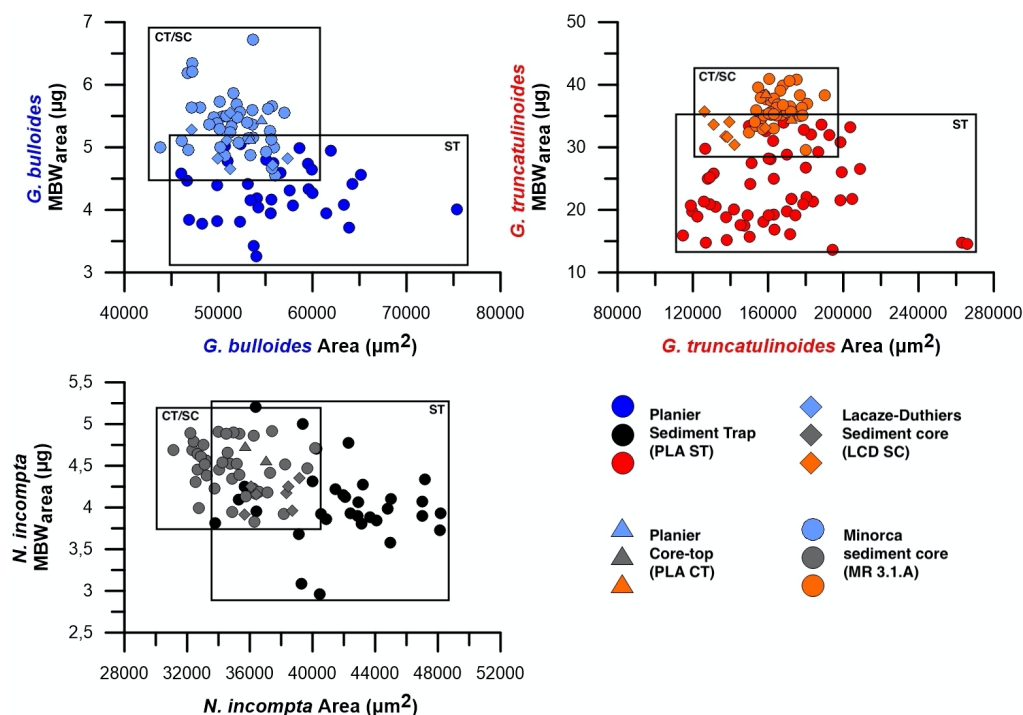


713 dwellers are unaffected by recent ocean acidification and changes in the carbonate
714 system and that the recent change in one or several environmental drivers may be
715 stimulating the calcification of these species.

716 Here, we theorize that the interannual patterns presented in Figure 5 mainly reflect
717 the seasonal changes in the regional oceanographic setting. As described previously
718 (see study area), the Gulf of Lions is influenced by a strong seasonality. The recent
719 SST decrease could be linked to an enhancement in water mixing, as cold and deep
720 salty water reach up to the surface. This mechanism would be less intense during
721 years 2000 to 2002, corresponding to a SST increase along with a salinity decrease
722 and absolute minimums in nutrients concentrations (Figure 5), as water stratifies,
723 these are consumed by primary production. Finally, in recent years, water mixing
724 seems to be reactivated, as SST keeps decreasing and nutrients concentrations
725 increase again. This mechanism also affects the carbonate system parameters, as
726 water mixing brings to surface deeper DIC enriched waters to the surface, coupled
727 with a $[\text{CO}_3^{2-}]$ reduction. Our data shows that alkalinity patterns display similar
728 tendencies to DIC, however, until the second time span covered by carbonate
729 system data, alkalinity variations are proportionally higher than DIC variations (see
730 Supplementary material), suggesting a water mixing phenomenon. On the other
731 hand, DIC variations turn to be higher than alkalinity variations from 2003 to 2005,
732 suggesting an additional effect of carbon inputs on the carbonate system not
733 reflected in the alkalinity data.

734

735 **5.3. Holocene core-top data comparison**



736
737

Figure 6. MBW_{area} in µg and area in µm² comparison in the sediment trap (PLA ST), Planier core-top (PLA CT), and both Lacaze-Duthiers (LCD SC) and Minorca sediment core (MR 3.1.A). Darker colors represent data from the sediment trap, while lighter colors represent data from the different seabed sediments.

741
742

743 The comparison of the well-preserved assemblages of planktic foraminifera in the
744 Holocene-aged surface sediments with those collected by a long-sediment trap
745 record offers a unique opportunity to assess the impact of recent environmental
746 change on the calcification of calcareous zooplankton in the Mediterranean Sea.
747 However, when comparing data from sediment traps and seabed sediments, the
748 possible role of calcite dissolution must be taken into account.

749 Calcite dissolution in the water column and/or on the sea floor could be invoked as
750 a source of variability between the sediment trap and surface sediment data sets
751 (e.g., Dittert et al., 1999). Therefore, in order to obtain meaningful interpretations
752 from our data sets it is important to assess the possible role of dissolution in the
753 preservation of planktic foraminifera shells. Several lines of evidence suggest,
754 however, that calcite preservation does not represent an important source of bias in
755 our study area. Firstly, the Mediterranean Sea is supersaturated with respect to
756 calcite (Millero et al., 1979) and the location of all the analyzed samples is much
757 shallower than the location of the calcite saturation horizon (Álvarez et al., 2014),



758 therefore, calcite dissolution seems unlikely (Schneider et al., 2007). Secondly,
759 several sediment trap studies have documented that calcareous plankton
760 experience negligible dissolution in their transit from the surface ocean to the sea
761 floor (Beaufort et al., 2007; Moy et al., 2009; Rigual-Hernández et al., 2020). Thirdly,
762 if partial dissolution was to take place here, MBWs from the seabed sediments and
763 core tops would be lighter than the ones from the sediment traps, which is not the
764 case (Figure 6). Fourthly, SEM observations of all 3 species in samples from the
765 sediment traps showed no sign of dissolution and foraminifera were well preserved
766 (see Supplementary material). All these arguments suggest that calcite dissolution
767 does not represent an important control in the weight of the planktic foraminifer shells
768 in the analyzed samples.

769 Overall, the lower shell weights of the foraminifera collected by the traps strongly
770 suggest that the three planktic foraminifera species have experienced a reduction in
771 their calcification since the industrial era and/or late Holocene. While the shell weight
772 of each species measured in the sediments show some variability across seabed
773 sediments (Figure 6), our data suggest an overall reduction of 18-24% for *G.*
774 *bulloides*, 20-27% for *N. incompta*, and 32-40% for *G. truncatulinoides*. It is important
775 to note that the range of shell weight variability across core-tops and sediment cores
776 (4.5-6.7 μg and 0.37 μg typical deviation for *G. bulloides*, 3.8-4.9 μg and 0.23 μg
777 typical deviation for *N. incompta*, and 29.5-40.9 μg and 2.6 μg typical deviation for *G.*
778 *truncatulinoides*) is substantially lower than the difference with the sediment trap
779 data (3-5 μg and 0.5 μg typical deviation for *G. bulloides*, 2.9-5.2 μg and 0.5 μg
780 typical deviation for *N. incompta* and 12-35 μg and 6 μg typical deviation for *G.*
781 *truncatulinoides*), implying that the shell weight of modern foraminifera populations
782 for the three species is lower than anywhere in the NW Mediterranean in the pre-
783 industrial times. The source of the variability across core tops and sediment cores is
784 most likely caused by the different age of the samples, ranging from 1979 years at
785 Minorca mid-depth (see section 3.1.) sample to 460 years at Planier core-top sample
786 and the different environments associated to the location of each core top.

787 Something to consider when comparing recent sediment trap data with pre-industrial
788 Holocene data is the life cycle of the species. As all the species analyzed presented
789 some reduction in shell calcification, the degree to which the different specimens
790 responded varied. The greatest weight reductions were observed for *G.*
791 *truncatulinoides* populations, while *G. bulloides* populations exhibited the lowest
792 weight loss.

793 Previous work stated that those species hosting photosynthetic algal symbionts
794 exhibit a higher tolerance to environmental changes that may affect their calcification
795 (Lombard et al., 2009). This is due to the fact that these symbionts can modify the
796 sea water chemistry that is close range to the shell, allowing a calcification



797 enhancement. Since none of the species studied here are symbiont bearing species,
798 they are among the most vulnerable foraminifera species to any sea water chemistry
799 change. Moy et al., (2009) work in the Southern Ocean, showed a 30-35%
800 calcification reduction for *G. bulloides* during the industrial era. Our study shows that
801 such a similar reduction in *G. bulloides* MBW_{area} (i.e., a mean 20% taking into
802 account the 3 sites studied) has also taken place in the Mediterranean Sea. Even
803 though the species studied were different in Fox et al., (2020), and that shell
804 thickness was analyzed, that work showed a massive shell reduction for *N. dutertrei*
805 (around 75%) and a smaller reduction for *G. ruber* (around 20%). *N. incompta* weight
806 reduction in this study is around 25%, despite that life cycles are different between
807 these species, our results come in the same line. Data for *G. truncatulinoides*
808 calcification comparison between pre-industrial Holocene and post-industrial
809 Holocene is scarce. One of the few available studies is the one of Pallacks et al.,
810 (2020) in the western Mediterranean sea using pre-industrial data and recent
811 foraminifera weight data obtained from high resolution core-tops. Size-normalized
812 weights showed that all the species calcification decreased since the onset of the
813 industrial revolution, an observation that is supported by our data (Figure 6). *G.*
814 *truncatulinoides* showed a 24% weight reduction, which is a lower reduction than
815 what is shown in our study (around 35% MBW_{area} decrease), but shows a similar
816 trend. Taken together, all these observations suggest that a decrease in major
817 planktic foraminifera calcification is not a regional feature but a global scale process.
818 Therefore, it is likely that global changes in the ocean, such as ocean acidification,
819 could be the main responsible for such a change.

820 6. Conclusions

821

822 The variability in shell calcification of three planktic foraminifera species (*Globigerina*
823 *bulloides*, *Neogloboquadrina incompta* and *Globorotalia truncatulinoides*) was
824 studied in the northwestern Mediterranean Sea at different time scales using
825 sediment trap and seabed samples. The analysis of 273 samples and more than
826 4000 individuals revealed that:

- 827 i. The Sieve Based Weight (SBW) method is not a reliable tool as
828 calcification indicator due to the influence of morphometric parameters on
829 foraminifera weight. The Measured Based Weight (MBW) technique, on
830 the other hand, shows little to negligible influence of the morphometric
831 parameters, and therefore, can be considered a reliable calcification
832 proxy.
- 833 ii. Analysis of the seasonal variability of planktic foraminifera calcification
834 revealed important differences between species. *G. bulloides* exhibited



835 peak calcification during winter, *N. incompta* during mid-summer and *G.*
836 *truncatulinoidea* during late summer to autumn. Correlations with
837 environmental parameters indicate that Optimum Growth Conditions
838 (OGC), Sea Surface Temperatures (SST) and $[\text{CO}_3^{2-}]$ are the most likely
839 parameters influencing seasonal calcification variability in the Gulf of
840 Lions.

841 iii. Interannual analysis suggest that *G. bulloidea* and *N. incompta* tend to
842 show a slight calcification reduction from 1994 to 2005, on the other hand,
843 *G. truncatulinoidea* displays a constant and steady calcification increase
844 over the years.

845 iv. Finally, sediment trap and seabed sediment data comparisons between
846 pre-industrial and post-industrial foraminifera assemblages. Our data
847 shows that all three species experienced a clear and conspicuous
848 calcification reduction with modern *G. bulloidea* populations being 18-24%
849 less calcified and a reduction of 20-27% and 32-40% for *N. incompta* and
850 *G. truncatulinoidea*, respectively.

851 As planktic foraminifera represent roughly about 50% of pelagic calcite production
852 (Schiebel, 2002) in the world's oceans, and therefore, an important component of
853 the marine carbon cycle, a reduction in the calcification of their shell could induce
854 important changes in the future carbon cycle with feed-backs on climate. Our results
855 call for increasing efforts in monitoring planktic foraminifera calcification the
856 Mediterranean in order to determine if the trends suggested by our data will be
857 sustained over time.

858
859 The Supplement related to this article is available at...

860
861 *Competing interests.* The authors declare that they have no conflict of interest.

862 *Author contributions.* ASRH, FJS and TMB designed the study and performed the numerical
863 analyses. JPT designed Figures 1 and 2. XDM provided Planier core-top and Lacaze-
864 Duthiers seabed sediment samples. IC provided the Minorca promontory seabed sediment
865 samples. NH and TE carried out the ^{14}C measurements. TMB led the sample processing as
866 well as the microscopy and image analysis, the foraminifera study and wrote the manuscript
867 with feedback from all authors.

868 *Acknowledgments.* Authors would like to thank Blanca Ausín for her insight on radiocarbon
869 dating and Serge Heussner for the retrieval of the sediment trap collected within the French
870 national MOOSE program supported by CNRS-INSU and ALLENI. This study was funded
871 by by the Spanish "Ministerio de Ciencia e Innovación" through a grant number PRE2019-
872 089091 and through the project RTI2018-099489-B-100; PID2021-128322NB-I00.



873 References

- 874 Aldridge, D., Beer, C.J., Purdie, D.A., 2012. Calcification in the planktonic foraminifera
875 *Globigerina bulloides*; linked to phosphate concentrations in surface waters of the North
876 Atlantic Ocean. *Biogeosciences* 9, 1725–1739. <https://doi.org/10.5194/bg-9-1725-2012>
- 877 Álvarez, M., Sanleón-Bartolomé, H., Tanhua, T., Mintrop, L., Luchetta, A., Cantoni, C.,
878 Schroeder, K., Civitarese, G., 2014. The CO₂ system in the Mediterranean Sea: a basin
879 wide perspective. *Ocean Sci.* 10, 69–92. <https://doi.org/10.5194/os-10-69-2014>
- 880 Barker, S., Elderfield, H., 2002. Foraminiferal Calcification Response to Glacial-Interglacial
881 Changes in Atmospheric CO₂. *Science* 297, 833–836.
882 <https://doi.org/10.1126/science.1072815>
- 883 Barker, S. & Ridgwell, A. Ocean Acidification. *Nature Education Knowledge* 3(10), 2 (2012).
- 884 Beaufort, L., Probert, I., Buchet, N., 2007. Effects of acidification and primary production on
885 coccolith weight: Implications for carbonate transfer from the surface to the deep ocean.
886 *Geochemistry, Geophysics, Geosystems* 8.
- 887 Beer, C. J., Schiebel, R., Wilson, P.A., 2010. Technical Note: On methodologies for determining
888 the size-normalised weight of planktic foraminifera. *Biogeosciences* 7, 2193–2198.
889 <https://doi.org/10.5194/bg-7-2193-2010>
- 890 Beer, Christopher J., Schiebel, R., Wilson, P.A., 2010. Testing planktic foraminiferal shell weight
891 as a surface water [CO₂] proxy using plankton net samples. *Geology* 38, 103–106.
892 <https://doi.org/10.1130/G30150.1>
- 893 Béranger, K., Mortier, L., Gasparini, G.-P., Gervasio, L., Astraldi, M., Crépon, M., 2004. The
894 dynamics of the Sicily Strait: a comprehensive study from observations and models. *Deep*
895 *Sea Research Part II: Topical Studies in Oceanography* 51, 411–440.
896 <https://doi.org/10.1016/j.dsr2.2003.08.004>
- 897 Bethoux, J.P., Gentili, B., Morin, P., Nicolas, E., Pierre, C., Ruiz-Pino, D., 1999. The
898 Mediterranean Sea: a miniature ocean for climatic and environmental studies and a key for
899 the climatic functioning of the North Atlantic. *Progress in Oceanography* 44, 131–146.
900 [https://doi.org/10.1016/S0079-6611\(99\)00023-3](https://doi.org/10.1016/S0079-6611(99)00023-3)
- 901 Bethoux JP, Boukhary MS, Ruiz-Pino D, Morin P, Copin Montegut C (2005) Nutrient, Oxygen
902 and Carbon Ratios, CO₂ sequestration and anthropogenic forcing in the Mediterranean
903 Sea. *Hdb Environment Chemical*, 5, 67–86.
- 904 Burke, J.E., Renema, W., Henehan, M.J., Elder, L.E., Davis, C.V., Maas, A.E., Foster, G.L.,
905 Schiebel, R., Hull, P.M., 2018. Factors influencing test porosity in planktonic foraminifera.
906 *Biogeosciences* 15, 6607–6619. <https://doi.org/10.5194/bg-15-6607-2018>
- 907 Canals, M., Puig, P., de Madron, X.D., Heussner, S., Palanques, A., Fabres, J., 2006. Flushing
908 submarine canyons. *Nature* 444, 354–357. <https://doi.org/10.1038/nature05271>
- 909 Chapman, M.R., 2010. Seasonal production patterns of planktonic foraminifera in the NE Atlantic
910 Ocean: Implications for paleotemperature and hydrographic reconstructions: CURRENTS.
911 *Paleoceanography* 25. <https://doi.org/10.1029/2008PA001708>
- 912 Cisneros, M., Cacho, I., Frigola, J., Canals, M., Masqué, P., Martrat, B., Casado, M., Grimalt,
913 J.O., Pena, L.D., Margaritelli, G., Lirer, F., 2016. Sea surface temperature variability in the
914 central-western Mediterranean Sea during the last 2700 years: a multi-proxy and multi-
915 record approach. *Clim. Past* 12, 849–869. <https://doi.org/10.5194/cp-12-849-2016>
- 916 Cléroux, C., Lynch-Stieglitz, J., Schmidt, M.W., Cortijo, E., Duplessy, J.-C., 2009. Evidence for
917 calcification depth change of *Globorotalia truncatulinoides* between deglaciation and
918 Holocene in the Western Atlantic Ocean. *Marine Micropaleontology* 73, 57–61.
919 <https://doi.org/10.1016/j.marmicro.2009.07.001>
- 920 de Moel, H., Ganssen, G.M., Peeters, F.J.C., Jung, S.J.A., Kroon, D., Brummer, G.J.A., Zeebe,
921 R.E., 2009. Planktic foraminiferal shell thinning in the Arabian Sea due to anthropogenic
922 ocean acidification? 9.



- 923 de Villiers, S., 2004. Optimum growth conditions as opposed to calcite saturation as a control on
924 the calcification rate and shell-weight of marine foraminifera. *Marine Biology* 144, 45–49.
925 <https://doi.org/10.1007/s00227-003-1183-8>
- 926 Demes, K.W., Bell, S.S., Dawes, C.J., 2009. The effects of phosphate on the biomineralization
927 of the green alga, *Halimeda incrassata* (Ellis) Lam. *Journal of Experimental Marine Biology*
928 *and Ecology* 374, 123–127. <https://doi.org/10.1016/j.jembe.2009.04.013>
- 929 Dickson, A.G., 1990. Standard potential of the reaction: $\text{AgCl(s)} + \text{H}^+(\text{g}) = \text{Ag(s)} + \text{HCl(aq)}$, and
930 and the standard acidity constant of the ion HSO_4^- in synthetic sea water from 273.15 to
931 318.15 K 15.
- 932 Dickson, A.G., Millero, F.J., 1987. A comparison of the equilibrium constants for the dissociation
933 of carbonic acid in seawater media 11.
- 934 Dittert, N., Baumann, K.-H., Bickert, T., Henrich, R., Huber, R., Kinkel, H., Meggers, H., 1999.
935 Carbonate dissolution in the deep-sea: methods, quantification and paleoceanographic
936 application, Use of proxies in paleoceanography. Springer, pp. 255-284.
- 937 Doney, S.C., Fabry, V.J., Feely, R.A., Kleypas, J.A., 2009. Ocean Acidification: The Other CO₂
938 Problem. *Annu. Rev. Mar. Sci.* 1, 169–192.
939 <https://doi.org/10.1146/annurev.marine.010908.163834>
- 940 Durrieu de Madron, X., Houpert, L., Puig, P., Sanchez-Vidal, A., Testor, P., Bosse, A., Estournel,
941 C., Somot, S., Bourrin, F., Bouin, M.N., Beauverger, M., Beguery, L., Calafat, A., Canals,
942 M., Cassou, C., Coppola, L., Dausse, D., D’Ortenzio, F., Font, J., Heussner, S., Kunesch,
943 S., Lefevre, D., Le Goff, H., Martín, J., Mortier, L., Palanques, A., Raimbault, P., 2013.
944 Interaction of dense shelf water cascading and open-sea convection in the northwestern
945 Mediterranean during winter 2012: shelf cascading and open-sea convection. *Geophys.*
946 *Res. Lett.* 40, 1379–1385. <https://doi.org/10.1002/grl.50331>
- 947 Durrieu de Madron, X., Ramondenc, S., Berline, L., Houpert, L., Bosse, A., Martini, S., Guidi, L.,
948 Conan, P., Curttil, C., Delsaut, N., Kunesch, S., Ghiglione, J.F., Marsaleix, P., Pujó-Pay, M.,
949 Séverin, T., Testor, P., Tamburini, C., the ANTARES collaboration, 2017. Deep sediment
950 resuspension and thick nepheloid layer generation by open-ocean convection: bnl
951 generation by open-ocean convection. *J. Geophys. Res. Oceans* 122, 2291–2318.
952 <https://doi.org/10.1002/2016JC012062>
- 953 Durrieu de Madron, X., Zervakis, V., Theocharis, A., Georgopoulos, D., 2005. Comments on
954 “Cascades of dense water around the world ocean.” *Progress in Oceanography* 64, 83–90.
955 <https://doi.org/10.1016/j.pocean.2004.08.004>
- 956 Estrada, M., Marrasé, C., Latasa, M., Berdalet, E., Delgado, M., Riera, T., 1993. Variability of
957 deep chlorophyll maximum characteristics in the Northwestern Mediterranean. *Mar. Ecol.*
958 *Prog. Ser.* 92, 289–300. <https://doi.org/10.3354/meps092289>
- 959 Fox, L., Stukins, S., Hill, T., Miller, C.G., 2020. Quantifying the Effect of Anthropogenic Climate
960 Change on Calcifying Plankton. *Sci Rep* 10, 1620. <https://doi.org/10.1038/s41598-020-58501-w>
- 961
- 962 Hassoun, A. E. R., Gemayel, E., Krasakopoulou, E., Goyet, C., Abboud-Abi Saab, M., Guglielmi,
963 V., Touratier, F. and Falco, C.: Acidification of the Mediterranean Sea from anthropogenic
964 carbon penetration, *Deep Sea Res. Part I Oceanogr. Res. Pap.*, 102, 1–
965 15, doi:10.1016/J.DSR.2015.04.005, 2015.
- 966 Hemleben, C., Spindler, M., Anderson, O.R., 1989. Modern Planktic Foraminifera.
- 967 Heussner, S., Durrieu de Madron, X., Calafat, A., Canals, M., Carbonne, J., Delsaut, N.,
968 Saragoni, G., 2006. Spatial and temporal variability of downward particle fluxes on a
969 continental slope: Lessons from an 8-yr experiment in the Gulf of Lions (NW
970 Mediterranean). *Marine Geology* 234, 63–92.
971 <https://doi.org/10.1016/j.margeo.2006.09.003>
- 972 Houpert L., X. Durrieu de Madron, P. Testor, A. Bosse, F. D’Ortenzio, M.N. Bouin, D. Dausse,
973 H. Le Goff, S. Kunesch, M. Labaste, L. Coppola, L. Mortier, P. Raimbault(2016)



- 974 Observations of open-ocean deep convection in the NorthwesternMediterranean Sea
975 seasonal and interannual variability of mixing and deep water masses for the 2007-2013
976 period. *Journal of Geophysical Research - Oceans*. doi : 10.1002/2016JC011857
977 IPCC, 2022. The Ocean and Cryosphere in a Changing Climate: Special Report of the
978 Intergovernmental Panel on Climate Change, 1st ed. Cambridge University Press.
979 <https://doi.org/10.1017/9781009157964>
980 Jonkers, L., Hillebrand, H., Kucera, M., 2019. Global change drives modern plankton
981 communities away from the pre-industrial state. *Nature* 570, 372–375.
982 <https://doi.org/10.1038/s41586-019-1230-3>
983 Kiss, P., Jonkers, L., Hudáčková, N., Reuter, R.T., Donner, B., Fischer, G., Kucera, M., 2021.
984 Determinants of Planktonic Foraminifera Calcite Flux: Implications for the Prediction of
985 Intra- and Inter-Annual Pelagic Carbonate Budgets. *Global Biogeochem Cycles* 35.
986 <https://doi.org/10.1029/2020GB006748>
987 Kroeker, K.J., Kordas, R.L., Crim, R., Hendriks, I.E., Ramajo, L., Singh, G.S., Duarte, C.M.,
988 Gattuso, J., 2013. Impacts of ocean acidification on marine organisms: quantifying
989 sensitivities and interaction with warming. *Glob Change Biol* 19, 1884–1896.
990 <https://doi.org/10.1111/gcb.12179>
991 Kuroyanagi, A., Kawahata, H., 2004. Vertical distribution of living planktic foraminifera in the seas
992 around Japan. *Marine Micropaleontology* 53, 173–196.
993 <https://doi.org/10.1016/j.marmicro.2004.06.001>
994 Lazzari, P., Mattia, G., Solidoro, C., Salon, S., Crise, A., Zavatarelli, M., Oddo, P. and Vichi, M.:
995 The impacts of climate change and environmental management policies on the trophic
996 regimes in the Mediterranean Sea: Scenario analyses, *J. Mar. Syst.*, 135, 137–
997 149, doi:10.1016/j.jmarsys.2013.06.005, 2014.
998 Lejeusne C, Chevaldonné P, Pergent-Martini C, Boudouresque CF, PérezT(2009) Climate
999 change effects on a miniature ocean: the highly diverse, highly impacted Mediterranean
1000 Sea. *Trends in Ecology & Evolution*, 25, 250–260.
1001 Lirer, F., Sprovieri, M., Vallefucio, M., Ferraro, L., Pelosi, N., Giordano, L., Capotondi, L., 2014.
1002 Planktic foraminifera as bio-indicators for monitoring the climatic changes that have
1003 occurred over the past 2000 years in the southeastern Tyrrhenian Sea. *Integrative Zoology*
1004 9, 542–554. <https://doi.org/10.1111/1749-4877.12083>
1005 Lombard, F., da Rocha, R.E., Bijma, J., Gattuso, J.-P., 2010. Effect of carbonate ion
1006 concentration and irradiance on calcification in planktic foraminifera. *Biogeosciences* 7,
1007 247–255. <https://doi.org/10.5194/bg-7-247-2010>
1008 Lombard, F., Erez, J., Michel, E., Labeyrie, L., 2009. Temperature effect on respiration and
1009 photosynthesis of the symbiont-bearing planktic foraminifera *Globigerinoides ruber* ,
1010 *Orbulina universa* , and *Globigerinella siphonifera*. *Limnol. Oceanogr.* 54, 210–218.
1011 <https://doi.org/10.4319/lo.2009.54.1.0210>
1012 Lombard, F., Labeyrie, L., Michel, E., Bopp, L., Cortijo, E., Retailleau, S., Howa, H., Jorissen, F.,
1013 2011. Modelling planktic foraminifer growth and distribution using an ecophysiological multi-
1014 species approach. *Biogeosciences* 8, 853–873. <https://doi.org/10.5194/bg-8-853-2011>
1015 Loulergue, L., Parrenin, F., Blunier, T., 2007. New constraints on the gas age-ice age difference
1016 along the EPICA ice cores, 0–50 kyr. *Clim. Past* 14.
1017 Lüthi, D., Le Floch, M., Bereiter, B., Blunier, T., Barnola, J.-M., Siegenthaler, U., Raynaud, D.,
1018 Jouzel, J., Fischer, H., Kawamura, K., Stocker, T.F., 2008. High-resolution carbon dioxide
1019 concentration record 650,000–800,000 years before present. *Nature* 453, 379–382.
1020 <https://doi.org/10.1038/nature06949>
1021 Margaritelli, G., 2020. *Globorotalia truncatulinoides* in Central - Western Mediterranean Sea
1022 during the Little Ice Age. *Marine Micropaleontology* 11.
1023 Marshall, B.J., Thunell, R.C., Henehan, M.J., Astor, Y., Wejnert, K.E., 2013. Planktic
1024 foraminiferal area density as a proxy for carbonate ion concentration: A calibration study



- 1025 using the Cariaco Basin ocean time series: foraminiferal area density [CO₃²⁻] proxy.
1026 *Paleoceanography* 28, 363–376. <https://doi.org/10.1002/palo.20034>
- 1027 Marty, J.-C., Chiavérini, J., Pizay, M.-D., Avril, B., 2002. Seasonal and interannual dynamics of
1028 nutrients and phytoplankton pigments in the western Mediterranean Sea at the DYFAMED
1029 time-series station (1991–1999). *Deep Sea Research Part II: Topical Studies in*
1030 *Oceanography* 49, 1965–1985. [https://doi.org/10.1016/S0967-0645\(02\)00022-X](https://doi.org/10.1016/S0967-0645(02)00022-X)
- 1031 Mehrbach, C., Culberson, C.H., Hawley, J.E., Pytkowicz, R.M., 1973. Measurement of the
1032 apparent dissociation constants of carbonic acid in seawater at atmospheric pressure.
1033 *Limnol. Oceanogr.* 18, 897–907. <https://doi.org/10.4319/lo.1973.18.6.0897>
- 1034 Meier, K.J.S., Beaufort, L., Heussner, S., Ziveri, P., Université, A.-M., 2014. The role of ocean
1035 acidification in *Emiliana huxleyi* coccolith thinning in the Mediterranean Sea 13.
1036 *Biogeosciences*, 11, 2857–2869, 2014. <https://doi:10.5194/bg-11-2857-2014>
- 1037 Millero, F.J., Morse, J., Chen, C.-T., 1979. The carbonate system in the western Mediterranean
1038 sea. *Deep Sea Research Part A. Oceanographic Research Papers* 26, 1395-1404.
- 1039 Millot, C., 1999. Circulation in the Western Mediterranean Sea. *Journal of Marine Systems* 20,
1040 423–442. [https://doi.org/10.1016/S0924-7963\(98\)00078-5](https://doi.org/10.1016/S0924-7963(98)00078-5)
- 1041 Millot, C., 1991. Mesoscale and seasonal variabilities of the circulation in the western
1042 Mediterranean. *Dynamics of Atmospheres and Oceans* 15, 179–214.
1043 [https://doi.org/10.1016/0377-0265\(91\)90020-G](https://doi.org/10.1016/0377-0265(91)90020-G)
- 1044 Monaco A., X. Durrieu de Madron, O. Radakovitch, S. Heussner & J. Carbonne (1999). Origin
1045 and variability of downward biogeochemical fluxes on the Rhone continental margin (NW
1046 Mediterranean)). *Deep-Sea Research I*, 46: 1483-1512.
- 1047 Moy, A.D., Howard, W.R., Bray, S.G., Trull, T.W., 2009. Reduced calcification in modern
1048 Southern Ocean planktic foraminifera. *Nature Geosci* 2, 276–280.
1049 <https://doi.org/10.1038/ngeo460>
- 1050 Nguyen, T.M.P., Petrizzo, M.R., Speijer, R.P., 2009. Experimental dissolution of a fossil
1051 foraminiferal assemblage (Paleocene–Eocene Thermal Maximum, Dababiya, Egypt):
1052 Implications for paleoenvironmental reconstructions. *Marine Micropaleontology* 73, 241–
1053 258. <https://doi.org/10.1016/j.marmicro.2009.10.005>
- 1054 Orr, J.C., Fabry, V.J., Aumont, O., Bopp, L., Doney, S.C., Feely, R.A., Gnanadesikan, A., Gruber,
1055 N., Ishida, A., Joos, F., Key, R.M., Lindsay, K., Maier-Reimer, E., Matear, R., Monfray, P.,
1056 Mouchet, A., Najjar, R.G., Plattner, G.-K., Rodgers, K.B., Sabine, C.L., Sarmiento, J.L.,
1057 Schlitzer, R., Slater, R.D., Totterdell, I.J., Weirig, M.-F., Yamanaka, Y., Yool, A., 2005.
1058 Anthropogenic ocean acidification over the twenty-first century and its impact on calcifying
1059 organisms. *Nature* 437, 681–686. <https://doi.org/10.1038/nature04095>
- 1060 Osborne, E.B., Thunell, R.C., Marshall, B.J., Holm, J.A., Tappa, E.J., Benitez-Nelson, C., Cai,
1061 W., Chen, B., 2016. Calcification of the planktic foraminifera *Globigerina bulloides* and
1062 carbonate ion concentration: Results from the Santa Barbara Basin. *Paleoceanography* 31,
1063 1083–1102. <https://doi.org/10.1002/2016PA002933>
- 1064 Paasche, E. and Brubank, S.: Enhanced calcification in the coccolithophorid *Emiliana huxleyi*
1065 (*Haptophyceae*) under phosphorus limitation, *Phycologia*, 22, 324–330, 1994.
- 1066 Pallacks, S., Anglada-Ortiz, G., Belen Martrat, P. Graham Mortyn, Grelaud, M., Incarbona, A.,
1067 Schiebel, R., Garcia-Orellana, J., Ziveri, P., 2020. Western Mediterranean marine cores
1068 show that foraminiferal mass and flux are being influenced by enhanced anthropogenic
1069 pressure. <https://doi.org/10.13140/RG.2.2.26245.99045>
- 1070 Parrenin, F., Jouzel, J., Kawamura, K., Lemieux-Dudon, B., Loulergue, L., Masson-Delmotte, V.,
1071 Narcisi, B., Raisbeck, G., Raynaud, D., Ruth, U., Schwander, J., Severi, M., Spahni, R.,
1072 Steffensen, J.P., Svensson, A., Udisti, R., Waelbroeck, C., Wolff, E., 2007. The EDC3
1073 chronology for the EPICA Dome C ice core. *Clim. Past* 13.



- 1074 Pujol, C., Grazzini, C.V., 1995. Distribution patterns of live planktic foraminifers as related to
1075 regional hydrography and productive systems of the Mediterranean Sea. *Marine*
1076 *Micropaleontology* 25, 187–217. [https://doi.org/10.1016/0377-8398\(95\)00002-1](https://doi.org/10.1016/0377-8398(95)00002-1)
1077 Rigual-Hernández, A.S., Sierro, F.J., Bárcena, M.A., Flores, J.A., Heussner, S., 2012. Seasonal
1078 and interannual changes of planktic foraminiferal fluxes in the Gulf of Lions (NW
1079 Mediterranean) and their implications for paleoceanographic studies: Two 12-year
1080 sediment trap records. *Deep Sea Research Part I: Oceanographic Research Papers* 66,
1081 26–40. <https://doi.org/10.1016/j.dsr.2012.03.011>
1082 Rigual-Hernández, A.S., Trull, T.W., Flores, J.A., Nodder, S.D., Eriksen, R., Davies, D.M.,
1083 Hallegraeff, G.M., Sierro, F.J., Patil, S.M., Cortina, A., Ballegeer, A.M., Northcote, L.C.,
1084 Abrantes, F., Rufino, M.M., 2020. Full annual monitoring of Subantarctic *Emiliania huxleyi*
1085 populations reveals highly calcified morphotypes in high-CO₂ winter conditions. *Scientific*
1086 *Reports* 10, 2594.
1087 Sabine, C.L., Feely, R.A., Gruber, N., Key, R.M., Lee, K., Bullister, J.L., Wanninkhof, R., Wong,
1088 C.S., Wallace, D.W.R., Tilbrook, B., Millero, F.J., Peng, T.-H., Kozyr, A., Ono, T., Rios, A.F.,
1089 2004. The Oceanic Sink for Anthropogenic CO₂. *Science* 305, 367–371.
1090 <https://doi.org/10.1126/science.1097403>
1091 Schiebel, R., 2002. Planktic foraminiferal sedimentation and the marine calcite budget: Marine
1092 calcite budget. *Global Biogeochem. Cycles* 16, 3-1-3–21.
1093 <https://doi.org/10.1029/2001GB001459>
1094 Schiebel, R., Hemleben, C., 2017. *Planktic Foraminifers in the Modern Ocean*. Springer Berlin
1095 Heidelberg, Berlin, Heidelberg. <https://doi.org/10.1007/978-3-662-50297-6>
1096 Schiebel, R., Hemleben, C., 2000. Interannual variability of planktic foraminiferal populations and
1097 test flux in the eastern North Atlantic Ocean (*JGOFs*) 44.
1098 Schiebel, R., Hemleben, C., n.d. *Modern planktic foraminifera* 14.
1099 Schiebel, R., Waniek, J., Zeltner, A., Alves, M., 2002. Impact of the Azores Front on the
1100 distribution of planktic foraminifers, shelled gastropods, and coccolithophorids. *Deep Sea*
1101 *Research Part II: Topical Studies in Oceanography* 49, 4035–4050.
1102 [https://doi.org/10.1016/S0967-0645\(02\)00141-8](https://doi.org/10.1016/S0967-0645(02)00141-8)
1103 Schiebel, R., Waniek, J., Bork, M., and Hemleben, C.: Planktic foraminiferal production
1104 stimulated by chlorophyll redistribution and entrainment of nutrients, *Deep-Sea Res. Pt. I*,
1105 48, 721–740, 2001.
1106 Schmidt, D. N., Renaud, S., Bollmann, J., Schiebel, R., and Thierstein, H. R.: Size distribution of
1107 Holocene planktic foraminifer assemblages: biogeography, ecology and adaptation, *Mar. Mi-*
1108 *cropaleontol.*, 5, 319–338, 2004.
1109 Schneider A, Tanhua T, Körtzinger A, Wallace DWR (2010) High anthropogenic carbon content
1110 in the eastern Mediterranean. *Journal of Geophysical Research*, 115, C12050.
1111 doi:10.1029/2010JC006171.
1112 Spero, H. J., Lerche, I., and Williams, D. F.: Opening the carbon isotope ‘vital effect’ box. 2.
1113 Quantitative model for interpreting foraminiferal carbon isotope data, *Paleoceanography*, 6,
1114 639655, 1991.
1115 Wacker L, Fülöp RH, Hajdas I, Molnár M, Rethemeyer J. 2013b. A novel approach to process
1116 carbonate samples for radiocarbon measurements with helium carrier gas. *Nuclear*
1117 *Instruments and Methods in Physics Research B* 294:214–7.
1118 Zarkogiannis, S.D., Iwasaki, S., Rae, J.W.B., Schmidt, M.W., Mortyn, P.G., Kontakiotis, G.,
1119 Hertzberg, J.E., Rickaby, R.E.M., 2022. Calcification, Dissolution and Test Properties of
1120 Modern Planktic Foraminifera From the Central Atlantic Ocean. *Front. Mar. Sci.* 9, 864801.
1121 <https://doi.org/10.3389/fmars.2022.864801>
1122 Zeppenfeld, K., 2019. Inhibition of calcite precipitation by orthophosphate at different water flow
1123 7.



1124 Ziveri P (2012) Research turns to acidification and warming in the Mediterranean Sea, IMBER
1125 (Integrated Marine Biogeochemistry and Ecosystem Research). News- letter, Issue 20,
1126 May 2012. <http://www.imber.info/index.php/News/Newsletters/Issue-n-20-May-2012>.